EPRI | ELECTRIC POWER RESEARCH INSTITUTE

Flow-Accelerated Corrosion – The Entrance Effect

1015072

Flow-Accelerated Corrosion – The Entrance Effect

1015072

Technical Update, November 2007

EPRI Project Manager

H. Crockett

ELECTRIC POWER RESEARCH INSTITUTE
3420 Hillview Avenue, Palo Alto, California 94304-1338 ▪ PO Box 10412, Palo Alto, California 94303-0813 ▪ USA
800.313.3774 ▪ 650.855.2121 ▪ askepri@epri.com ▪ www.epri.com

DISCLAIMER OF WARRANTIES AND LIMITATION OF LIABILITIES

ORGANIZATION(S) THAT PREPARED THIS DOCUMENT

Sequoia Consulting Group, Inc

This is an EPRI Technical Update report. A Technical Update report is intended as an informal report of continuing research, a meeting, or a topical study. It is not a final EPRI technical report.

NOTE

For further information about EPRI, call the EPRI Customer Assistance Center at 800.313.3774 or e-mail askepri@epri.com.

CITATIONS

This document was prepared by

Sequoia Consulting Group, Inc
163 Pleasant Street
Attleboro, MA 02703

Principal Investigator
J. Horowitz

This document describes research sponsored by the Electric Power Research Institute (EPRI).

This publication is a corporate document that should be cited in the literature in the following manner:

Flow-Accelerated Corrosion – The Entrance Effect. EPRI, Palo Alto, CA: 2007. 1015072.

PRODUCT DESCRIPTION

Flow-accelerated corrosion (FAC) is a degradation process that attacks carbon steel components and equipment in the steam and feedwater system of conventional and nuclear power plants. In the simplest terms, FAC can be considered as the dissolution of the normally protective iron oxide film into a flowing stream of water or a water-steam mixture. FAC occurs only when the fluid is moving, when it contains water, and when it is unsaturated in iron. FAC can, in fact, be modeled as a turbulent mass transfer process. This was the approach taken by Berge and his co-workers at Électricité de France.

Although reasonably well understood, in the 1990s a new effect was documented. This effect has been called the "leading edge effect" or, perhaps more properly, the "entrance effect" or "mass transfer entrance effect." This effect occurs when flow passes from an FAC-resistant material to a nonresistant (susceptible) material, which causes a local increase in the corrosion rate. This effect is normally manifested by a groove downstream of the attachment weld between the corroding and the resistant material. Although observed and identified in the 1990s, investigators had speculated about its existence since the early 1980s.

This investigation was undertaken to describe the effect, provide a mechanistic description, document plant experience, and quantify the effect. Recommendations to plant owners are also discussed.

Results and Findings

This report describes selected occurrences of the entrance effect in U.S. nuclear plants. Plant experience from three units is presented in detail. Other experience, anecdotal experience, and some speculation are also presented.

Additionally, the technical literature was examined, and relevant information was located. This information was used to develop numerical values for the enhancement produced as a function of system parameters. This set of values should be included in a future version of CHECWORKS™ Steam Feedwater Application.

Challenges and Objectives

Although programs to protect against FAC are in place in all domestic nuclear units, the entrance effect is not always incorporated into the inspection planning process. The objectives of this work were to describe the entrance effect and to quantify its magnitude.

Applications, Values, and Use

The results of this work will be used in future versions of the CHECWORKS™ Steam Feedwater Application. This improvement to the computer program will result in more accurate predictions of wear rate and will lead to an improved selection of inspection locations by utility engineers.

EPRI Perspective

Although often overlooked, the entrance effect may be important in determining the remaining service life of components. Further, FAC engineers should be aware of this effect to properly select inspection locations and to design repair measures. Eventually, this effect will be incorporated into CHECWORKS™.

This document will provide a single source of relevant information on the entrance effect.

Approach

A survey of CHECWORKS™ Users Group (CHUG) members was performed to determine examples of the entrance effect; additionally, a literature search was carried out to find analogous transport processes. With this assembled information, recommendations were developed.

Keywords

Flow-accelerated corrosion
FAC
Mass transfer
Single-phase flow
Two-phase flow

ACKNOWLEDGEMENTS

EPRI would like to acknowledge the contributions of the following individuals in support of this work.

- Andy Barth, South Carolina Electric and Gas
- Lee Goyette and Chris Beard, Pacific Gas and Electric
- Bob Montgomery, Public Service Electric & Gas.

EPRI also wishes to acknowledge Harold Crockett and Shane Findlan who sponsored this report.

CONTENTS

LIST OF FIGURES

LIST OF TABLES

1
INTRODUCTION

Flow-accelerated corrosion (FAC) is a degradation mechanism that affects carbon steel piping in power plant environments. It has caused a number of significant failures and the resultant degradation produced by FAC has necessitated numerous replacements in power plants worldwide. FAC is a well-known phenomenon that has been extensively documented (e.g., reference 1). FAC normally occurs in piping and equipment of the extraction steam, heater drains, and feedwater systems. In fact, FAC is the predominant degradation mechanism in these systems.

To deal with FAC caused degradation, computer programs such as CHECWORKS™ Steam Feedwater Application (SFA) (reference 2) have been developed. These programs use empirical relationships for various factors representing system parameters. These factors when combined result in a predicted rate of FAC. Although, FAC has been studied for more than 25 years, not all parametric effects are completely established.

An essential part of CHECWORKS™ SFA is the Chexal-Horowitz correlation that is used to predict the rate of FAC. This correlation has been under development since the late 1980s. The basis of the correlation is the large amount of both laboratory and plant data that has been assembled for benchmarking the correlation. Further information about the correlation is found in references 1, 2 and 3.

1.1 CHECWORKS™ SFA Correlation

An extensive body of experimental work has shown that the rate of FAC is governed by a number of parameters. For convenience, these parameters may be broken down in three groups, as follows:

- **Water Chemistry –** pH at temperature, and the oxygen concentration
- **Materials –** the chromium, copper and molybdenum concentration in the corroding material
- **Hydrodynamics –** the velocity, steam quality and local geometry.

Current theory (reference 1) holds that the hydrodynamic values are needed to model the mass transfer of iron species from the surface of the material to the free-stream of the flow. As mass transfer principles play an important part of this report, a brief explanation of mass transfer will be presented.

1.2 Mass Transfer

Mass transfer is the term used to describe processes that involve molecular and convective transport of atoms and molecules within physical systems. Mass transfer occurs in stationary (i.e., non-moving) systems, in laminar flow, and most commonly in turbulent flow.[1] Some examples of mass transfer processes are the evaporation of water from a pool; the diffusion of chemical impurities in oceans from point sources; and in cooling towers where evaporation of water cools that portion which remains as a liquid, as well as cooling and humidifying the air passing through.

The driving force for mass transfer is a difference in concentration. Microscopically, the random motion of molecules causes a net transfer of mass from an area of high concentration to an area of low concentration. The amount of mass transfer can be quantified through the calculation and application of mass transfer coefficients. Mass transfer finds wide application in chemical engineering practice. Petroleum refining and uranium enrichment are only two of many examples of industrial mass transfer. Finally, note that the topics of mass transfer, heat transfer and momentum transfer are often treated together due to similarities among them.

Moving from this general discussion to FAC, the iron species must be transferred from the steel and oxide surfaces to the flowing stream of water or water and steam. It is well known that geometries that increase turbulence (e.g., control valve, orifice) will increase the local rate of FAC. Note that under plant conditions the flow regime is virtually always turbulent.

1.3 Entrance Effect

It has been observed at a number of nuclear plants that the area immediately downstream of a weld will show accelerated wear under certain circumstances. In particular, if the weld connects resistant material (upstream) connecting non-resistant material (downstream) effect an area of increased wear will be apparent. See Figure 1-1 for a sample of such wear from the feedwater system at Diablo Canyon.

Consider this photograph; note that the flow is from right to left. The labeled area is carbon steel with enough trace chromium present to effectively inhibit FAC. Note the shiny, un-corroded appearance of this surface. Note also the two grooves on either side of this material. Theses are from the grinding done as part of the preparation for welding. Consider now, the material to the left of the weld. Note the roughened, corroded appearance. This material is carbon steel with only small amounts of trace alloy content. Now, note the area within the oval. This is the additional attack that is discussed in this report. The Diablo Canyon experience will be discussed in greater detail in Section 3 of this report.

---

[1] Laminar or streamline flow occurs at relatively low velocities. The motion of the fluid is smooth and regular and moves in parallel layers without mixing. In contrast, at higher velocities, the flow becomes chaotic with mixing prevalent within the fluid. This condition is known as turbulent flow.

The prediction of the transition between laminar and turbulent flow is most often made using the Reynolds number. The subject of flow regimes will be discussed in a later section of this report.

Note that similar enhancement is not shown at the downstream weld (i.e., the next weld that would be downstream of the left-hand side of Figure 1-1, whether or not resistant material is downstream. This fact rules out galvanic corrosion (i.e., corrosion due to dissimilar metals in contact). Further, similar wear is not shown if the metals connected by a weld are both non-resistant (susceptible). This rules out a pure geometric effect from the weld or the weld prepared area.

This type of wear was first described in a plant in reference 4, although, it is recognized that Coney postulated that such an effect would be observed under the appropriate conditions (reference 5). An excerpt from Coney's description of the phenomenon and another, very early, description of the effect are presented in Appendix A.

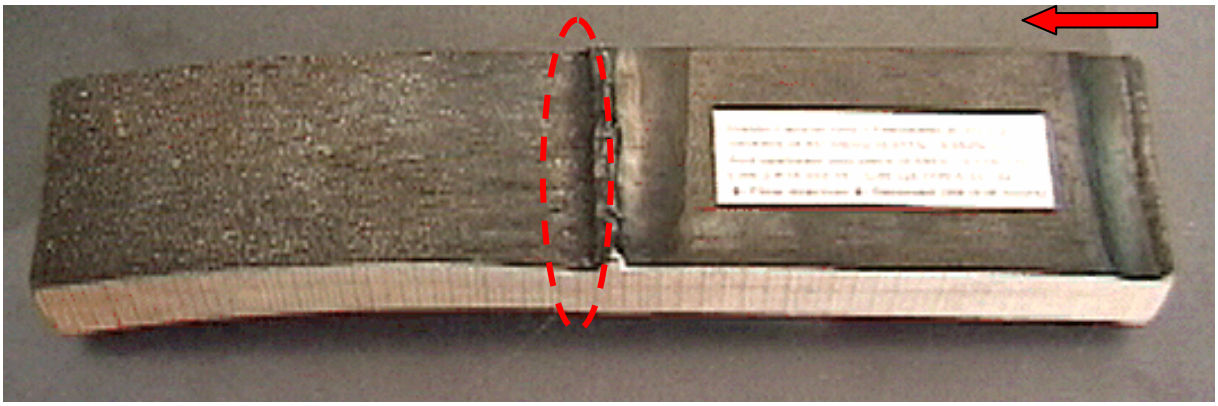

Figure 1-1
Sample from the Feedwater System at Diablo Canyon
(Photograph courtesy of Pacific Gas and Electric)

1.4 Report Overview

This report is organized as follows:

- Section 2 presents the objectives of this work,
- Section 3 describes the plant experience with the entrance effect,
- Section 4 introduces a mechanistic explanation of the effect,
- Section 5 presents correlations obtained from the technical literature,
- Section 6 presents a discussion of the implications of the entrance effect, and presents recommendations,
- Section 7 presents the references used.

Several appendices present further information.

2
OBJECTIVE

The objectives of this report are:

- Describe the experience with the entrance effect in nuclear power plants.
- Present a mechanistic explanation of this phenomenon.
- Provide an estimate of the augmentation of corrosion rate caused by this effect.
- Discuss plant implications.

3
PLANT EXPERIENCE

This section will describe plant experience with the entrance effect.

3.1 Diablo Canyon

Diablo Canyon is a two-unit pressurized water reactor site located on the central coast of California. In the mid nineteen nineties, there were a large number of inspections and replacements in the feedwater system. As part of the inspection program, trace chromium measurements were made using a spark tester. The materials measurement program is presented in reference 6.

During the replacement of a number of components, it was noted that there was a characteristic groove just downstream of the upstream weld. This grove occurred whenever the upstream material was resistant (i.e., contained trace chrome) and the downstream material was non-resistant (i.e., susceptible to FAC as it contained little or no trace chrome). This is illustrated in Figure 3-1 through Figure 3-5.

Considering these figures, the following comments are appropriate:

- Figure 3-1 is the same photograph as Figure 1-1. It shows a sample of a straight pipe (upstream) welded to a 90° elbow.
- Figure 3-2 shows a close-up of the previous photograph. Note that the downstream area shows corrosion while the upstream material is much less affected.
- The broken oval in Figure 3-3 clearly shows the downstream groove. Note the shallower upstream groove remaining from the weld prep.
- Figure 3-4 is a sketch showing measurements from one of the components replaced.
- Figure 3-5 is another photograph of the degradation found. The ruler shown is graduated in inches.

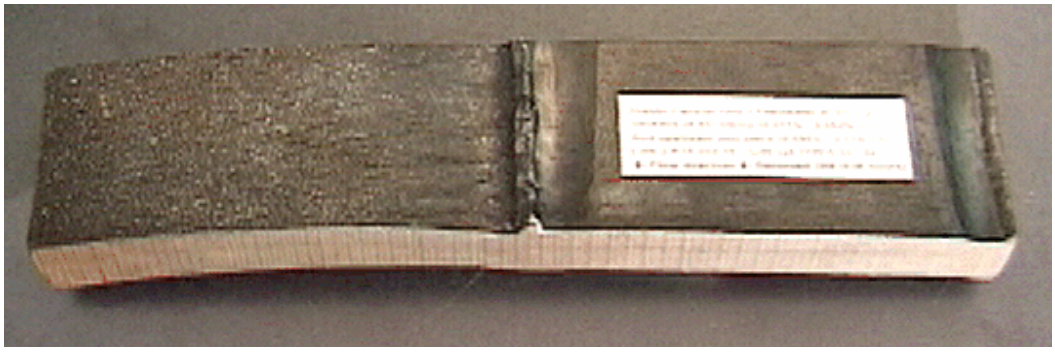

Figure 3-1
Overall View of Entrance Effect at Diablo Canyon
(Photograph courtesy of Pacific Gas & Electric)

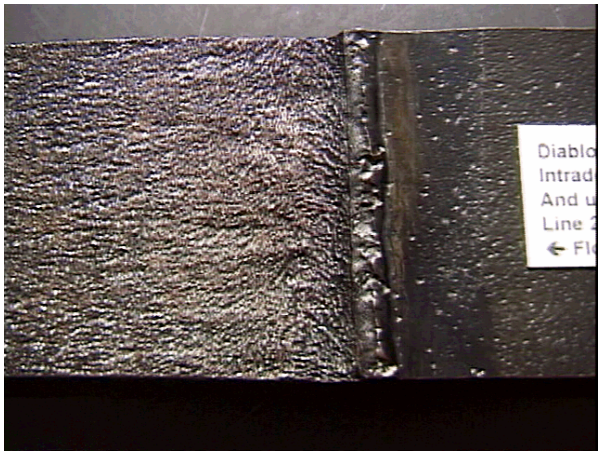

Figure 3-2
Close-up of the Weld Shown in Figure 3-1
(Photograph courtesy of Pacific Gas & Electric)

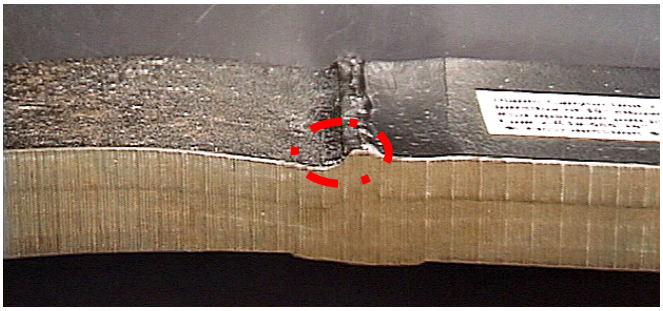

Figure 3-3
Side View of the Area Shown in Figure 3-1
(Photograph courtesy of Pacific Gas & Electric)

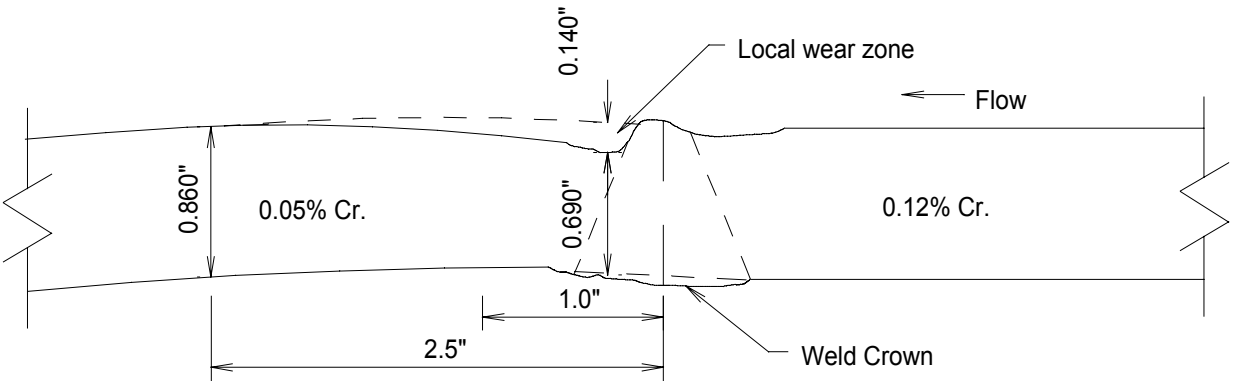

Figure 3-4
Sketch Showing the Typical Degradation Found
(Courtesy of Pacific Gas & Electric)

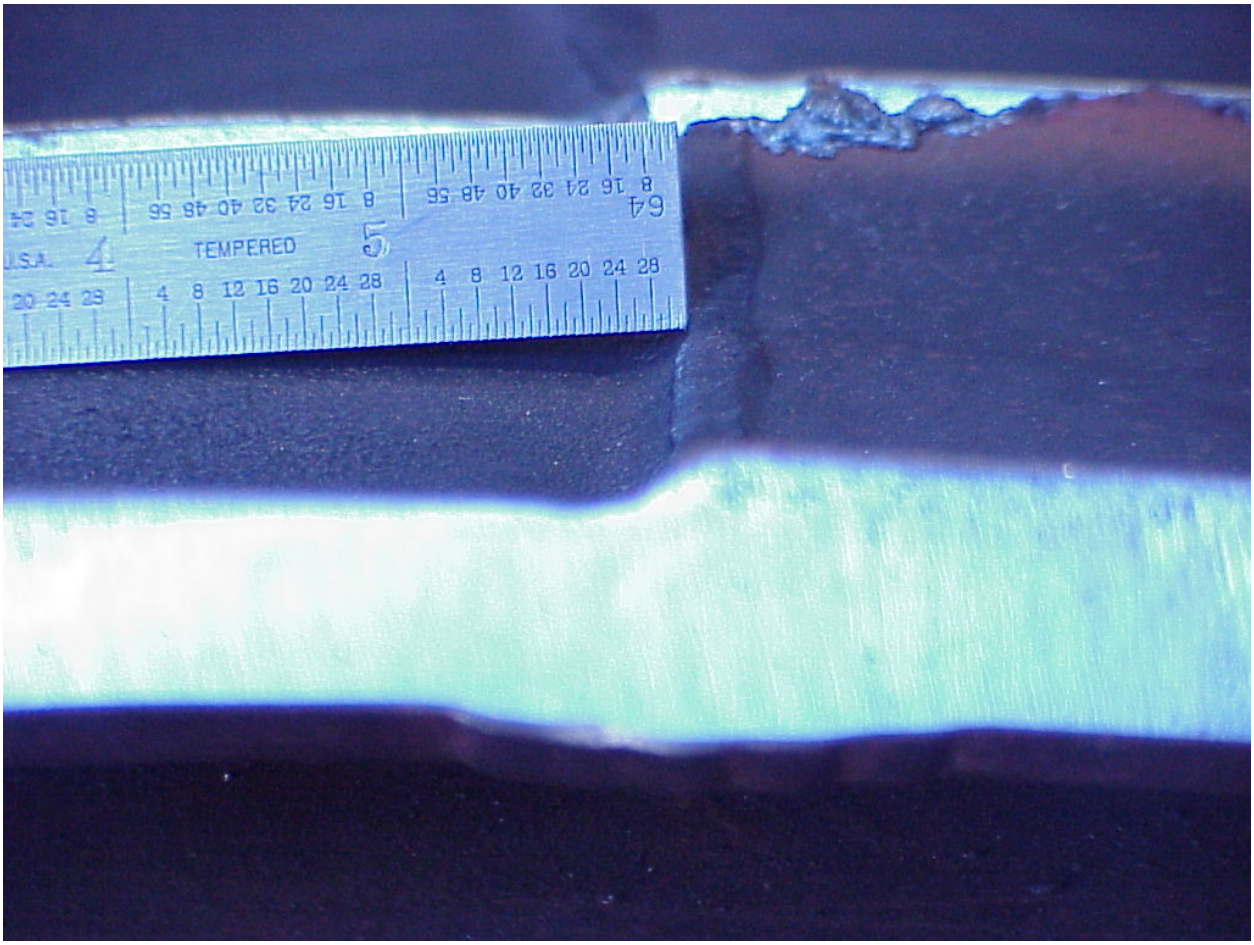

Figure 3-5
Photograph of Degradation Found (Photograph courtesy of Pacific Gas & Electric)

3.2 Salem

Salem is a two-unit PWR site located in southwestern New Jersey on Delaware Bay. In 2005, wear was found in a feedwater elbow. The elbow was 14-inch (355.6 mm) with a nominal thickness of 0.750 inch (19 mm). Note that for this size, 87.5% of the nominal thickness is 0.656 inch (16.7 mm). As inspected, the upstream portion of the elbow was thinned locally to a minimum thickness of 0.419 inch (10.65mm) or about 56% of the nominal thickness.

Figure 3-5 and 3-6 show the inside of this elbow with local measurements shown. Figure 3-7 presents a plot of refined grid readings using 1 inch (25.4 mm) squares in the area of interest. Note that the worst wear was at grid point I-1. The remainder of the elbow was much thicker with most readings near or above nominal.

The chromium in the upstream component and the affected elbow were measured to be 0.065% and 0.015% respectively (reference 7). Note that as was the case with Diablo Canyon, the entrance effect was caused by trace chrome in carbon steel material.

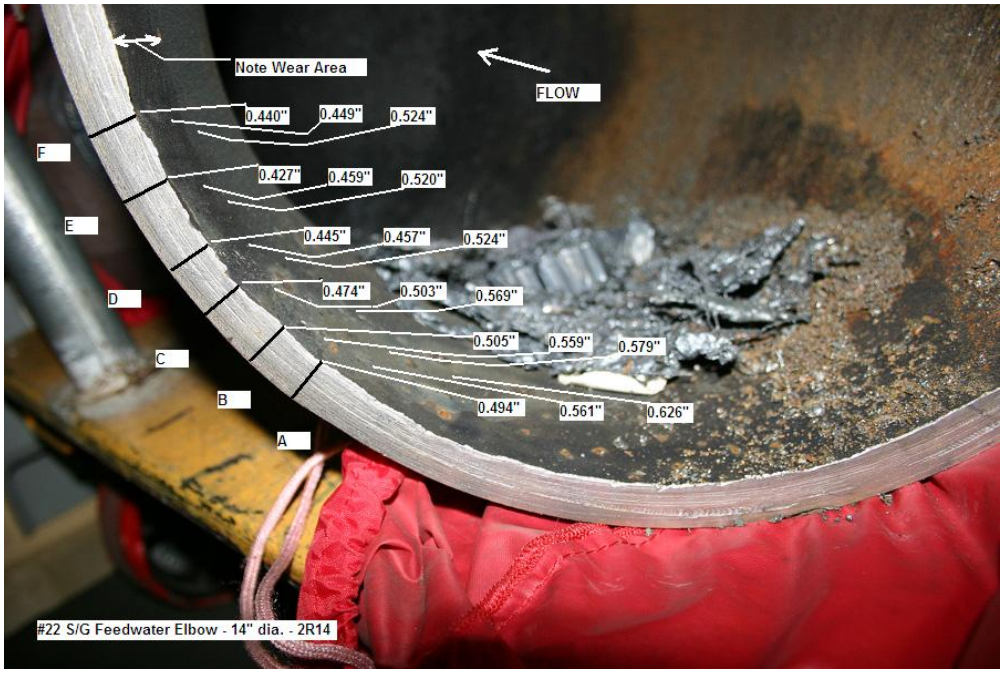

Figure 3-6
View Inside Salem Feedwater Elbow
(Photograph courtesy of Public Service Electric & Gas)

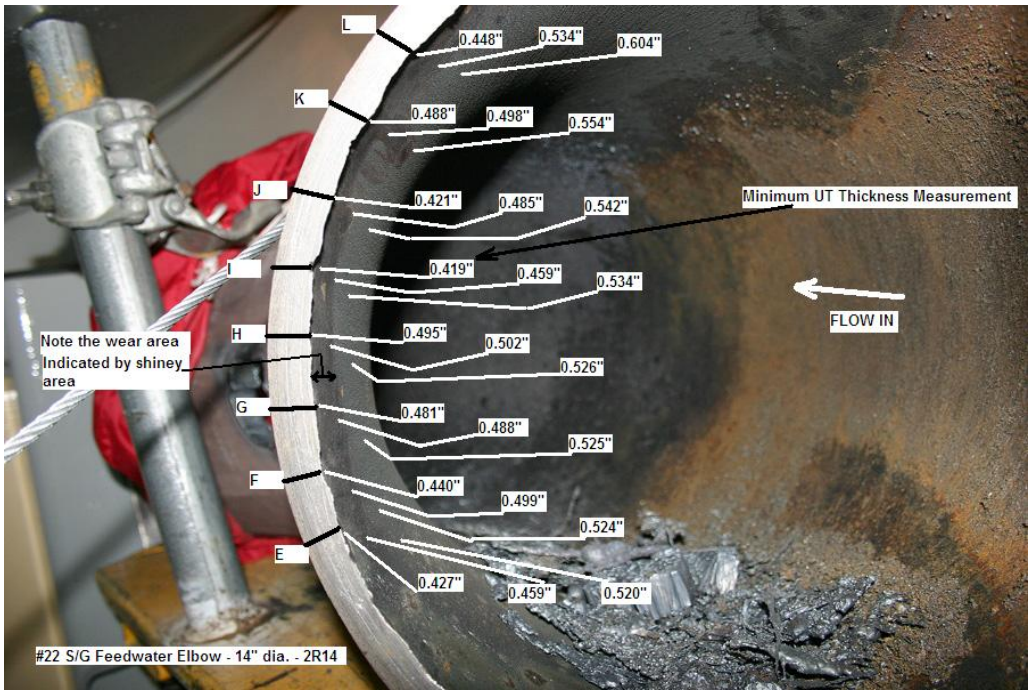

Figure 3-7
Another View inside Salem Feedwater Elbow
(Photograph courtesy of Public Service Electric & Gas)

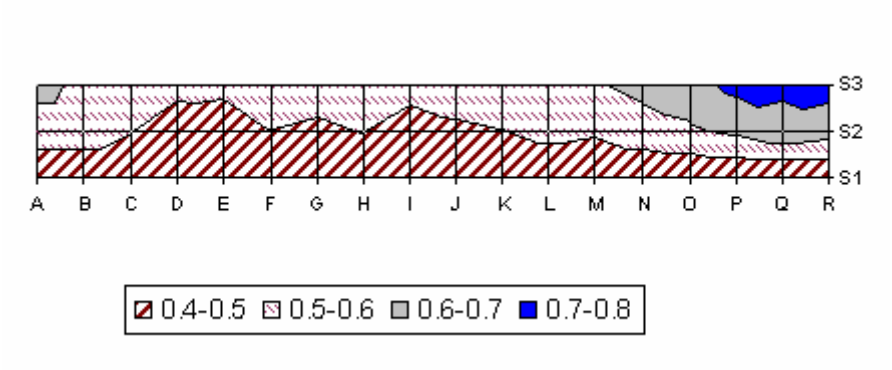

Figure 3-8
Grid Map of Salem Feedwater Elbow

3.3 V. C. Summer

V. C. Summer is a single-unit PWR site located in north central South Carolina. At the CHUG meeting in January 2007, a presentation was made describing the wear in an expander[2] (reference 8). The area in question consists of a valve followed by a 6 inch x 8 inch expander attached to another expander (8 inch x 16 inch), and then a pipe, see Figure 3-9. The inspection history of this area is presented in Table 3-1.

As can be seen from the table, there have been a number of inspections of the expander before and after the replacement of the upstream expander. What is striking is the difference in wear rate before and after the replacement of the upstream expander. The upstream expander was replaced because of high FAC wear. Comparing the measured minimum thickness for RF05 and RF07, little if any wear is occurring. Contrast that to the thickness measurements at RF12 and RF16, between these outages there is a linear wear rate of about 0.070 inch per cycle (1.77 mm/cycle). Note that this figure almost certainly over-states the wear rate as the two UT measurements were made closer to the weld in the second inspection. Regardless of that fact, the amount of degradation clearly increased after the installation of the new expander.

Figure 3-10 presents a cross-section of the replaced expander. Note that the labels on this figure. The larger (green) label represents the nominal thickness of the 8 inch end and the smaller (yellow) label represents the minimum acceptable thickness of the 8 inch end of the expander. Further note that the weld is not affected by FAC. This is normally the case although there are exceptions to this rule.

Table 3- 1
Inspection History of the Small End of the Expander at V. C. Summer

Outage	Minimum Measured Thickness – in (mm)	Comments
----	0.322 (8.43)	Nominal thickness of Schedule 40 expander
RF05	0.340 (8.64)	Measured thickness
RF07	0.349 (8.86)	Measured thickness – no wear
RF10	---	Upstream expander replaced with resistant material
RF12	0.293 (7.44)	Measured thickness
RF16	0.015 (0.38)	Component replaced

Note the outside diameter of the 8 inch end is 8.625 inch (219.1 mm) and the nominal thickness of this end is 0.322 inch (8.18 mm).

[2] An "expander" is the term used in the FAC community for a reducer with the flow from the small end to the large end. In other words a diffuser.

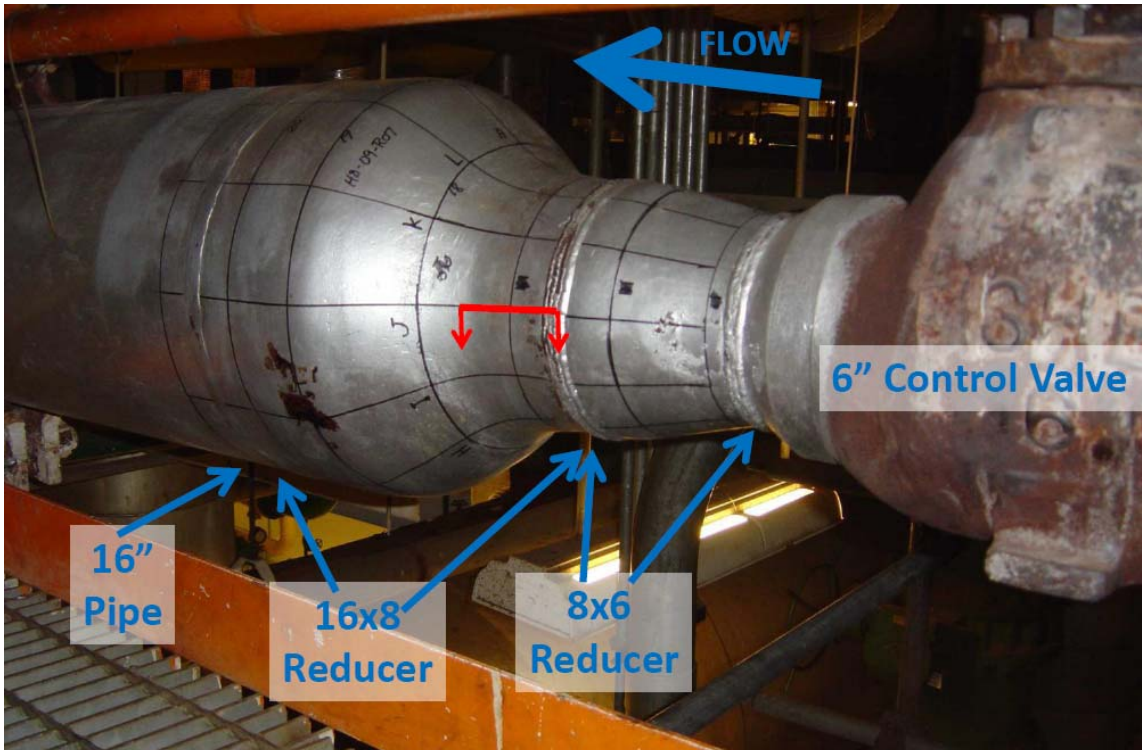

Figure 3-9
Photograph of the Piping at V. C. Summer (Photograph courtesy of South Carolina Electric & Gas)
Note the arrows on the reducer indicate the area of accelerated wear.

Figure 3-10
Cross Section of Expander at V. C. Summer
(Photograph courtesy of South Carolina Electric & Gas)

3.4 Other Examples of the Entrance Effect

The examples presented above are reasonably clear examples of the entrance effect. The examples presented in this section are less clear, but also likely examples.

3.4.1 Pleasant Prairie

The Pleasant Prairie Power Plant is a two-unit fossil station located in southeastern Wisconsin near Lake Michigan. In February 1995, a feedwater pipe failed catastrophically (see Figure 3-11). The failure occurred downstream of a tee immediately upstream of the entrance to the boiler. A sketch showing a top view of the accident location is presented in Figure 3-12.

Post accident investigation revealed that the pipe had a measured Chrome content of 0.03% and the tee had a measured Cr of 0.12%. This difference would be enough to cause the entrance effect immediately downstream of the weld attaching the branch pipe to the tee. This location is where the failure initiated. More details about this accident may be found in references 9,10.

Figure 3-11
Pleasant Prairie Power Plant Feedwater Pipe
(Photograph courtesy of Wisconsin Electric)

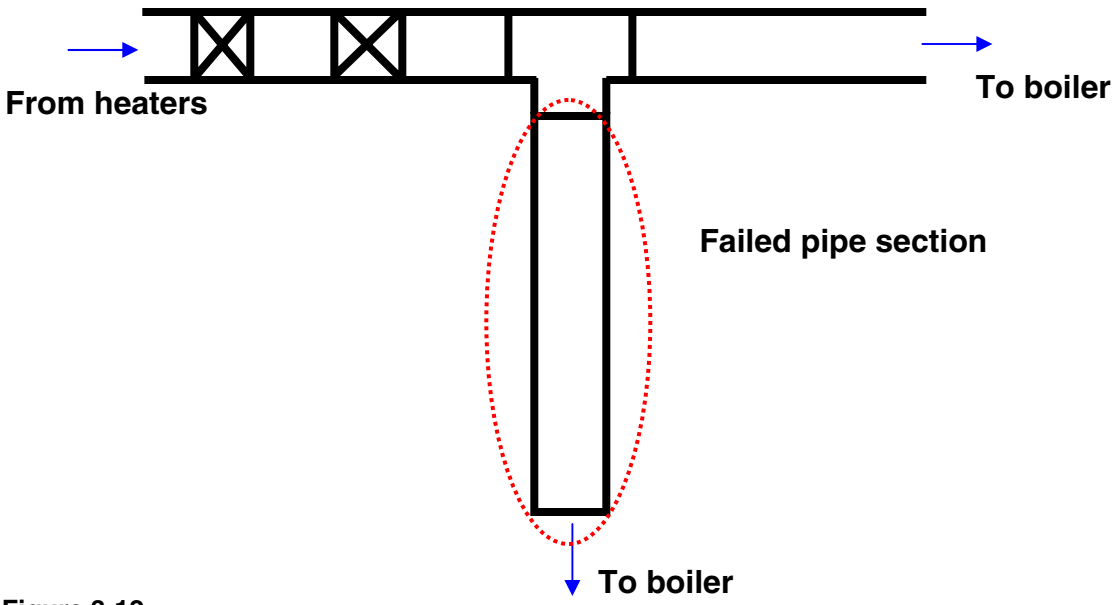

Figure 3-12
Top View of Pleasant Prairie Failure Location

3.4.2 Small Bore Failures

Two small bore failures will be discussed together.

V.C. Summer. In December 2004, a failure occurred in a 1 inch (25.4 mm) turbine casing drain (reference 11). The failure was in carbon steel pipe socket welded to a chrome moly coupling. See Figure 3-13. As the carbon steel piece was extensively thinned and damaged from the corrosion and during separation, it can only be assumed that the entrance effect played a part in this failure.

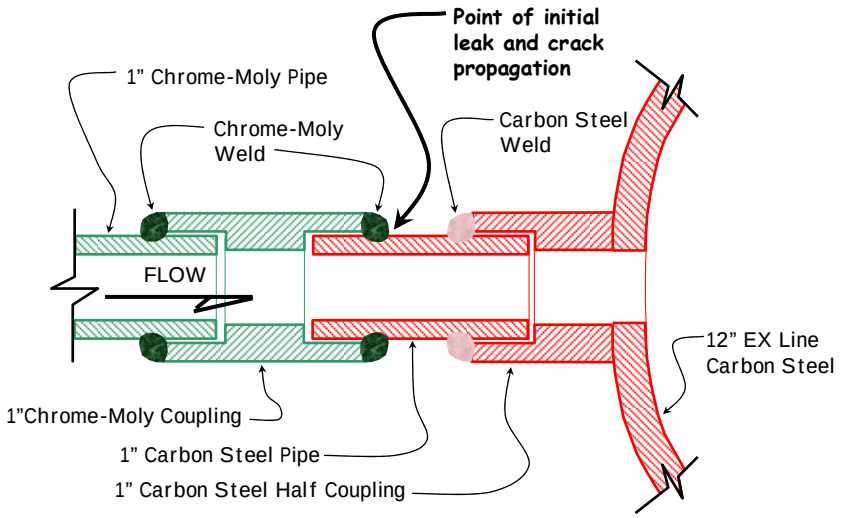

Figure 3-13
Sketch of Turbine Drain Line Failure at V. C. Summer

Diablo Canyon. In August 2005**,** a 2 inch, socket welded, vent pipe failed in a system that had been replaced with chrome-moly material (reference 12). Unfortunately, some of the carbon steel components were left in place and a leak resulted in a straight pipe. As can be seen in Figure 3-14, the edge of the carbon steel (left side of picture) was completely worn away.

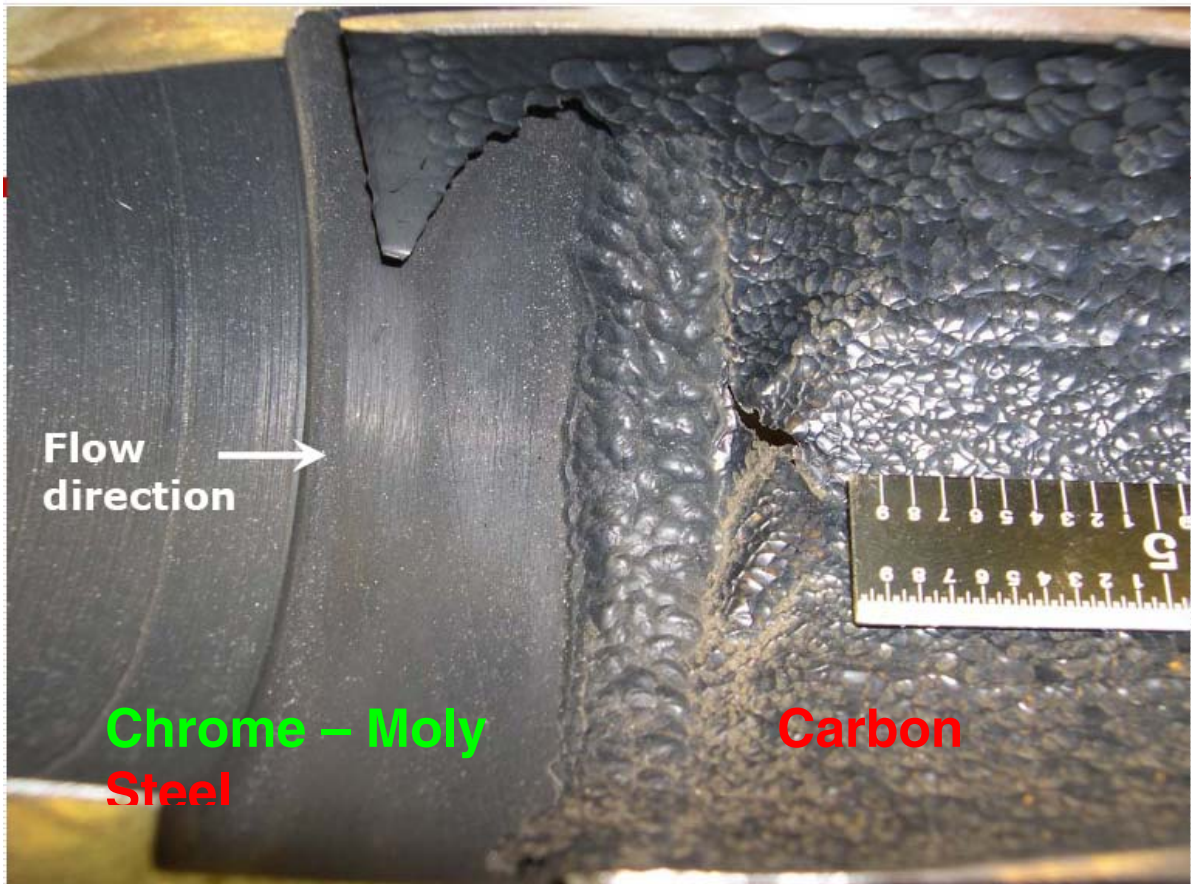

Figure 3-14
Internal View of Small Bore Leak at Diablo Canyon
(Photograph courtesy of Pacific Gas & Electric)

4
DESCRIPTION OF EFFECT

This section will present a description of the entrance effect. A more mechanistic description of this phenomenon is found in Appendix B. An alternate description using boundary layer analysis will be presented in Appendix C.

To describe the effect, turbulent mass transfer will be introduced.

4.1 Turbulent Mass Transfer

Let us consider flow of a fluid within a long straight pipe. If the velocity is low enough, the flow will be smooth, without internal mixing. This is type flow is known as "laminar" or "streamline" flow. As the velocity increases, a point will be reached where the flow begins a transition into a chaotic flow regime known as turbulent flow. Many experiments have shown that the transition regime begins at about a Reynolds number of 2,300 and is normally considered to be complete at a Reynolds number of 10,000. Note that the Reynolds number is a dimensionless number defined as:

$$\mathrm{Re} = \frac{\rho \cdot V \cdot L}{\mu} \qquad (4\text{-}1)$$

Where:

Re = Reynolds number
ρ = Liquid density
V = Velocity
L = Diameter (or characteristic length)
μ = Viscosity

In most power plant situations, the flow is well into the turbulent regime (i.e., Re >> 10,000).

In order to model FAC, we must consider turbulent mass transfer. Turbulent mass transfer occurs when a fluid in the turbulent regime, transfers mass with a solid surface. Typically, the amount of mass transfer that occurs is defined with a mass transfer coefficient.

$$h_D = \frac{w/A}{(C_o - C_\infty)} \qquad (4\text{-}2)$$

Where:

h_D = Mass transfer coefficient
w/A = Mass flux (mass flow rate per area)
C_o = Concentration of the species at the wall
C_∞ = Concentration of the species in the free-stream

There are a number of empirical correlations which have been proposed to relate mass transfer in straight pipes with turbulent flow with the operating conditions. Normally, these correlations are in terms of dimensionless numbers. For the purpose of this report, let us consider the Berger & Hau correlation (reference 13).

$$Sh = 0.0165 \cdot \mathrm{Re}^{0.86} \cdot Sc^{0.33} \qquad (4\text{-}3)$$

Where:

Sh = Sherwood Number (dimensionless)
Sc = Schmidt Number (dimensionless)[3]

The Sherwood and Schmidt numbers are defined as:

$$Sh = \frac{h_D \cdot D}{D_M} \qquad (4\text{-}4)$$

$$Sc = \frac{\mu}{\rho \cdot D_M} \qquad (4\text{-}5)$$

Where:

$\boldsymbol{D_M}$ = Mass diffusivity

Now, at the wall, the mass transfer is given by:

$$\frac{w}{A} = -D_M \cdot \left(\frac{\partial C}{\partial y} \right)_{y=0} \qquad (4\text{-}6)$$

This is a very important equation as it states that the concentration gradient at the wall governs the mass transfer. Note that the concentration gradient at the wall is the slope of the concentration profile at the wall.

Correlations, such as Berger & Hau are designed to predict to the mass transfer coefficient under a given set of operating conditions. Now, it is important to understand that these predictions are normally steady state in time and fully developed in space. Let us examine what these requirements imply.

- Steady state implies that there is no change with time. FAC is normally modeled as a steady state process as any changes with time will occur slowly, if at all.

- Spatially fully developed means that both the velocity profile and the mass transfer profile have reached conditions consistent with a long, undisturbed flow. The turbulent velocity profile is normally considered to be fully developed about 15 diameters downstream of an

[3] The significance of the Schmidt number will be discussed in the next section.

entrance or other disturbance.[4]

- The requirement that there is a fully developed concentration profile implies that the mass transfer has been taking place for a substantial distance upstream of the reference point such that the concentration profile for the mass being transferred (to or from the wall).

In any case, the steady-state, fully developed condition defines the smallest amount of mass transfer that can occur under a given set of conditions. Any perturbation results in more mass transfer (or in our case a higher corrosion rate).

4.2 Velocity and Concentration Profiles

If turbulent flow in a straight pipe is fully developed, the velocity profile will be as shown in Figure 4-1. This is the well known "bullet-shaped" profile. It is flatter than the laminar profile which is parabolic which is also shown in this figure.

When there is heat transfer to or from the fluid a similar situation arises. There is a distribution of temperature across the section of the pipe. This distribution is known as a temperature profile. Now, it is well known that the turbulent temperature profile (if there is heat transfer) and concentration profile (if there is mass transfer) will have a similar shape (see, for example reference 14). In other words, for the case of corroding carbon steel, the shape of the fully developed concentration profile would be similar to Figure 4-1 but with a high concentration near the wall and a lower concentration in mid-stream. This is illustrated in Figure 4-2.

Again, it should be stressed that these profiles represent fully developed in time and space profiles. In other words they would exist in a steady flow at the end of long straight, corroding pipe.

Finally, note that if there is no heat transfer to or from the wall, the temperature profile will be uniform across the pipe. Similarly, if there is no mass transfer, the concentration profile will be uniform across the pipe.

With this information, the mechanism behind the entrance effect will be described.

---

[4] Quoting reference 14 who is referring to the work of Deissler, "His results indicate that the local friction factors attain their fully developed values in much shorter lengths (roughly ten diameters from the inlet) than those required for the full development of the velocity profiles (known from experiment to exceed 50 diameters),

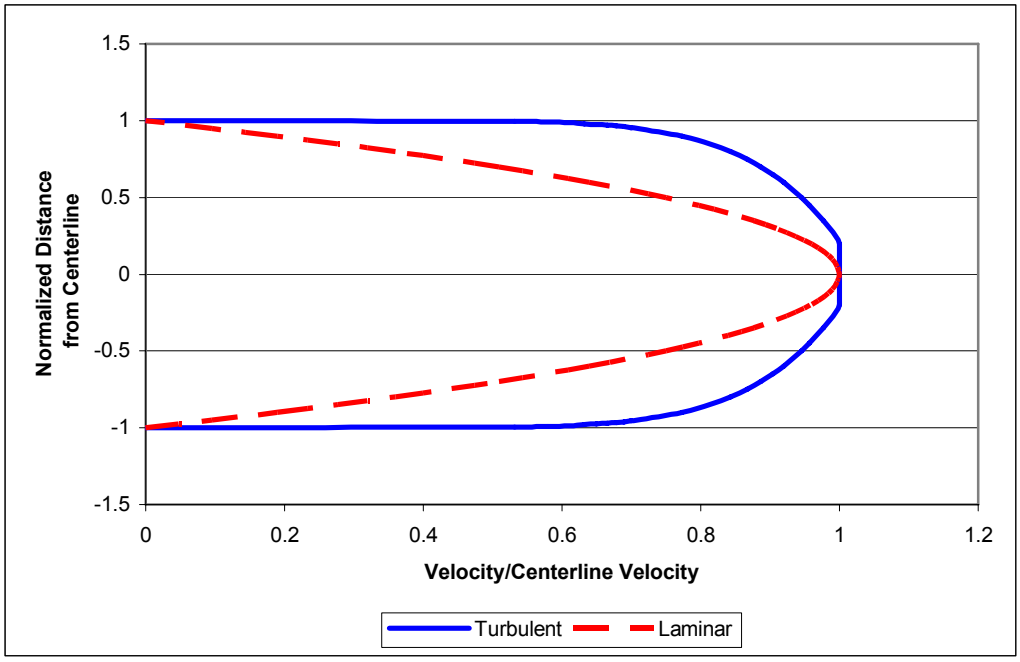

Figure 4-1
Fully Developed Velocity Profiles

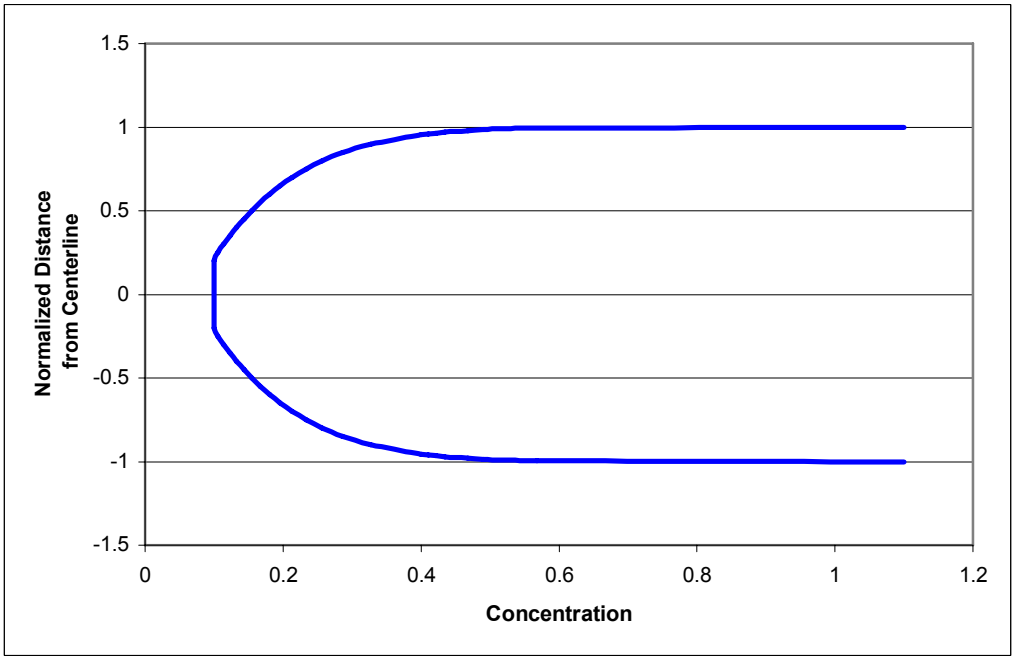

Figure 4-2
Fully Developed, Turbulent Concentration Profile

4.3 Entrance Effect

Consider two pipes welded together. The first pipe is made of resistant material (e.g., stainless steel) and the second pipe is made of non-resistant material (i.e., carbon steel). Assuming further, that the flow is from the resistant material to the susceptible material and that the resistant pipe is long enough that the velocity and concentration profiles at its exit are fully developed, we have defined the problem. With these assumptions the velocity profile is as illustrated in Figure 4-1 and the geometry for this case is illustrated in Figure 4-3.

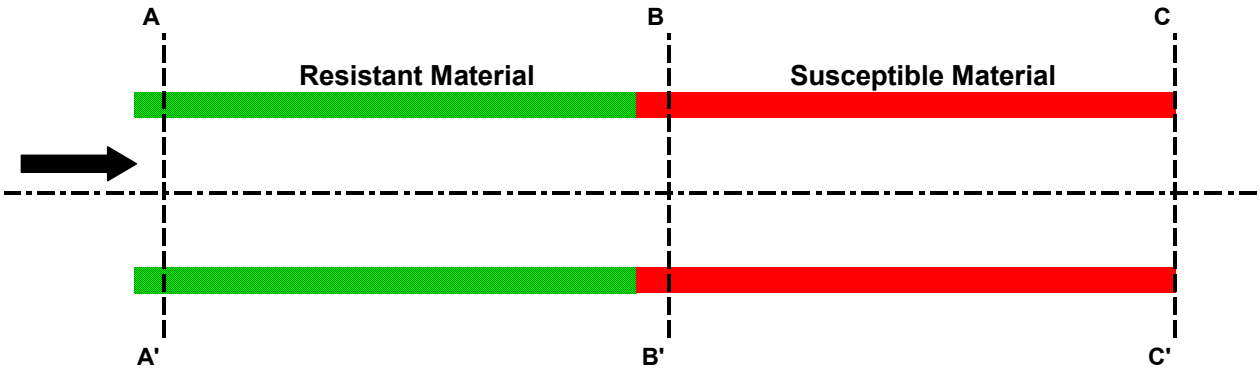

Figure 4-3
Schematic of Entrance Effect

Consider Figure 4-3, at Section A-A', the velocity profile should be similar to that of Figure 4-1. The concentration profile should be uniform, that is, constant across the section. At the other side of the figure, the concentration profile should be fully developed, say at Section C-C'. The concentration at this point would be similar to that shown in Figure 4-2.

The interesting location is just downstream of the joint between the resistant and the susceptible material, Section B-B'. At this location, the concentration profile is neither uniform, nor fully developed. Rather, it is something intermediate, see Figure 4-4. The portion of the profile near the wall shows that mass is being transferred to the fluid. However, the central portion of the flow is not yet affected by the wall. It is the necessary adjustment of the concentration profile that indicates that the entrance effect is occurring. Microscopically, the slope of the concentration profile at the wall goes from a mathematical singularity[5] at the interface between materials to the steady state value. Remember that the slope of the profile is a measure of the mass transfer.

[5] A mathematical singularity is a point at which a given mathematical function is not defined. In this case, the singularity exists, because there is a discontinuity in the concentration between the value of the wall and the fluid next to the wall. This discontinuity causes the derivative not to exist, and hence the rate of mass transfer is not defined.

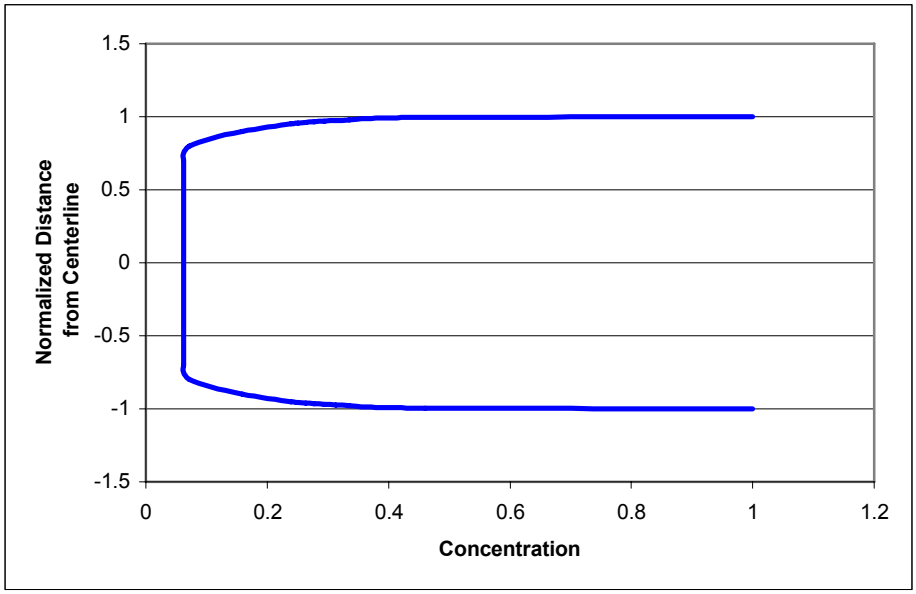

Figure 4-4
Developing Concentration Profile

4.4 An Analogous Example

The mathematical solution to the mass transfer problem will be discussed in the next section.

However, to close this section, some actual data from Hartnett (Reference 15) of an analogous heat transfer experiment will be presented. In his experiment, fluid flowed through a long, thermally insulated section. The upstream length was sufficient to generate a fully developed velocity profile. At a location denoted as zero, the insulation ended and heat was added to the fluid. Some of the results of this work are presented in Figure 4-5. Plotted is the heat transfer coefficient versus distance from the beginning of heat addition. The fluid in this figure was oil with a Reynolds number from 1,600 to 46,600 and a Prandtl number[6] that varied (because of temperature changes) from 48 to 390.

The data plotted for the two highest Reynolds number represent an analogous situation to the turbulent mass transfer situation being discussed.[7] Note that the heat transfer coefficient (analogous to the mass transfer coefficient) is indicative of the amount of heat being transferred, decays from values off the chart to the fully developed value in about 15 diameters. Note also that comparing the two highest Reynolds numbers, little effect of Reynolds number is apparent.

---

[6] The significance of the Prandtl number will discussed in the next section.

[7] The smallest two Reynolds numbers are clearly in the transition zone between laminar and turbulent flow and the middle Reynolds number (i.e. 10,100) is just outside of the transition regime.

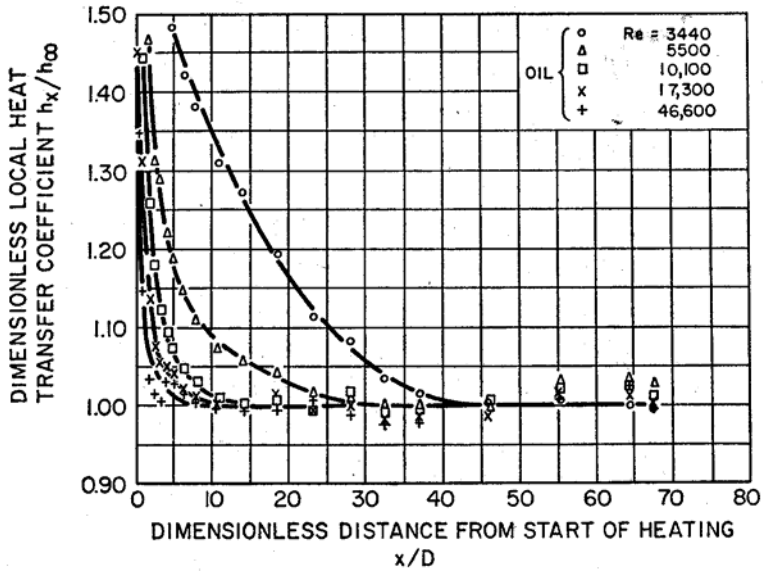

Figure 4-5
Thermal Entrance Effect, Data of Hartnett (Reference 15)

5
ANALYTICAL CONSIDERATIONS

5.1 Background

The technical literature was examined and no correlations and little work were found on solving the problem of the entrance effect on mass transfer. However, there was some information found on the analogous heat transfer problem. This work will now be summarized.

5.2 History

The problem of heat transfer with developing thermal conditions combined with an established velocity profile for laminar flow was defined and first solved by Graetz in the 1883 and later independently by Nusselt (reference 16). Because of this fact, the problem is known as the Graetz problem. These analyses showed that the temperature profile and the Nusselt number (i.e., the dimensionless number that contains the heat transfer coefficient) are functions of a dimensionless number (the Graetz number) defined as:

$$Gr = \frac{\mathrm{Re} \cdot \mathrm{Pr}}{(x/D)} \qquad (5\text{-}1)$$

Where:

Re = Reynolds number
Pr = Prandtl number
x = distance downstream of the insulated/heat transferring interface
D = pipe inside diameter

5.3 Prandtl Number and Schmidt Number

Before continuing, it is necessary to introduce the Prandtl number and the Schmidt number.

The Prandtl number is a dimensionless number defined as a ratio of physical properties ratio. Since it contains only properties, and for pure fluids, it is a function of only temperature. It is defined as:

$$\mathrm{Pr} = \frac{\nu}{\alpha} = \frac{\textit{viscous diffusion}}{\textit{thermal diffusion}} = \frac{C_p \cdot \mu}{k} \qquad (5\text{-}2)$$

where:

= kinematic viscosity, $= \mu /$.
= thermal diffusivity, $= k / (c_p)$
μ = dynamic viscosity.

k = thermal conductivity
= liquid density
C_p = specific heat at constant pressure

Typical values for Pr are:

- around 0.7 for air and many gases,
- around 1 for water at reasonably high temperatures
- between 100 and 40,000 for engine oil,
- around 0.015 for mercury

It is interesting to note that there are no known fluids with Prandtl numbers between gases (i.e., Pr ~ 0.7) and liquid metals (Pr < 0.02).

For convection, the Prandtl number describes which mode of heat transfer is more important. For a liquid metal such as mercury, heat conduction within the fluid is very effective compared to convection. Thus, conduction is dominant. Conversely, for engine oil, convection is very effective in transferring energy from an area, compared to pure conduction. Thus, momentum transport (convection) is dominant. For fluids with Prandtl numbers near unity, both mechanisms are important.

In heat transfer problems, the Prandtl number controls the relative thickness of the momentum and thermal boundary layers. If the Prandtl number is less than unity, then the thermal boundary layer is thicker than the momentum boundary layer. Conversely, the thermal boundary layer is thinner than the momentum boundary layer if the Prandtl number is greater than unity.

The mass transfer analog of the Prandtl number is the Schmidt number. The Schmidt number is a dimensionless number defined as the ratio of momentum diffusivity and mass diffusivity, and is used to characterize fluid flows in which there are simultaneous momentum and mass diffusion convection processes.

The Schmidt number relates the relative thickness of the hydrodynamic layer and mass-transfer boundary layer in an analogous way as Prandtl number does for heat transfer.
It is defined as:

$$Sc = \frac{\nu}{D_m} \qquad (5\text{-}3)$$

where:
= kinematic viscosity
D_m = mass diffusivity.

Note that the Schmidt number is not a property as is Prandtl number, rather the mass diffusivity depends on the combination of the fluid and the species being considered. In the case of FAC, the Schmidt number is about 6 at representative temperatures for iron species diffusing through water.

5.4 Turbulent Flow

The turbulent Graetz problem, i.e., the analogous problem of developing thermal conditions for a fully developed turbulent velocity profile, has been solved numerically by a number of investigators including Deissler (reference 17). These solutions are discussed in references 16, 18, 19 and 20. As should be expected the solution of the turbulent Graetz problem is more difficult than the laminar problem. Reference 20 presents a history of work performed in this area.

In view of the mathematical difficulties involved in the solution of these problems, numerical integration must be used. These results have been correlated by several investigators including – Reynolds, Al-Arabi, and the Engineering Sciences Data Unit (ESDU). These correlations will now be discussed.

Note that the form of this type of correlation often follows the results of the numerical solution. Reference 19 presents a form often used in this type of correlation as:

$$\frac{\overline{Nu}_D(x)}{\overline{Nu}_X(x=\infty)} = 1 + C_1\left(\frac{D}{x}\right)^{C_2} \qquad (5\text{-}4)$$

Where:

$\overline{Nu}$ = space averaged Nusselt Number[8]
C_1, C_2 = constants that may be a function or Reynolds and or Prandtl number

5.5 Available Correlations

This section will present three correlations for the turbulent entrance effect.

5.5.1 Reynolds

H.C. Reynolds[9] and co-workers developed a correlation for a Prandtl number of 0.71 corresponding to air and other gases. (This correlation is described in reference 20.) For our purposes, this correlation may be written as:

$$\frac{Nu_x}{Nu_\infty} = \frac{h_x}{h_\infty} = 1 + \frac{0.8\,(1 + 70{,}000\,\mathrm{Re}^{-1.5})}{x/D} \qquad (5\text{-}5)$$

Where:

---

[8] The Nusselt number is the heat transfer analog of the Sherwood number. It is defined as the heat transfer coefficient multiplied by the diameter divided by the thermal conductivity of the fluid.

[9] Not to be confused with Osborne Reynolds who the Reynolds number is named after.

Nu_x = Nusselt number at x
Nu_∞ = Nusselt number at infinity (i.e., fully developed conditions)
h_x = Heat transfer coefficient at x
h_∞ = Heat transfer coefficient at infinity (i.e., fully developed conditions)

Kakaç et al., (reference 20) state that this correlation agrees well with the data for x/D > 2.

5.5.2 Al-Arabi

Al-Arabi (reference 21) developed a correlation for the mean Nusselt number for a range of Prandtl numbers (0.7 to75). This correlation is in two parts:

$$\frac{\overline{Nu_m}}{\overline{Nu_\infty}} = \frac{\overline{h_m}}{\overline{h_\infty}} = 1 + \frac{C}{x/D} \tag{5-6}$$

Where:

$$C = \frac{(x/D)^{0.1}}{\mathrm{Pr}^{1/6}}\left(0.68 + \frac{3{,}000}{\mathrm{Re}^{0.81}}\right) \tag{5-7}$$

Kakaç et al., (reference 22), state that this correlation agrees well with the data for x/D > 2.

5.5.3 Engineering Sciences Data Unit

As quoted by Hewitt et al. (reference 22), the Engineering Sciences Data Unit has developed a correlation for the entrance region of gases (Prandtl number not given, but probably ~ 0.7).Note that there is no Reynolds number dependence, but the enhancement is a function of distance alone. This correlation is:

$$\frac{h_c}{h_\infty} = \frac{1}{0.113\ln(x/D) + 0.693} \tag{5-8}$$

Reference 22 states that the range of applicability of this correlation is 0.001 < x/D < 15.

5.6 Comparison of the Correlations

The above three correlations will be examined in two different way.

5.6.1 Prandtl Number Dependence

As the Al-Arabi correlation is the only one with a Prandtl number dependence, the predicted dependence on Prandtl number will be examined. As mentioned above, the Al-Arabi correlation is for fluids with Prandtl number between 0.7 and 75. Remember that for FAC the analogous Schmidt number is about 6.

Figure 5-1 presents the predictions of the Al-Arabi correlation at a Reynolds number of 100,000. As can be seen there is little impact of Prandtl number on the resultant enhancement. This conclusion is true at other Reynolds numbers.

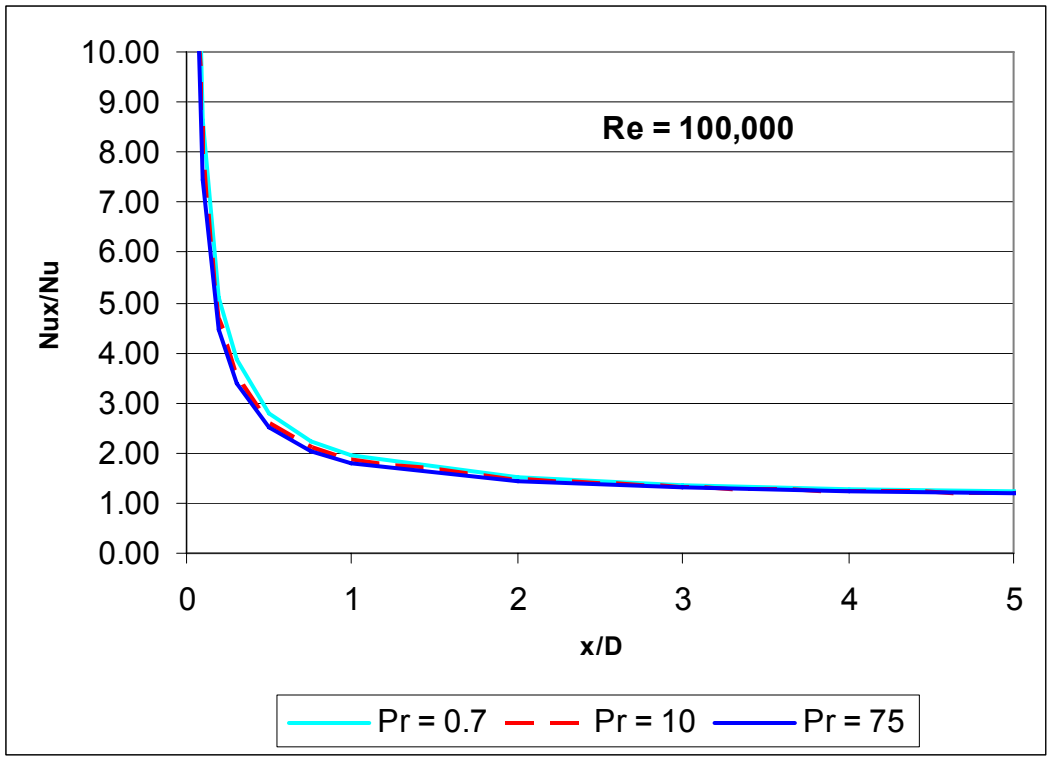

Figure 5-1
Prandtl Number Dependence of the Al-Arabi Correlation

5.6.2 Reynolds Number Dependence

As the Al-Arabi and Reynolds correlations have Reynolds number dependence, the two correlations will be examined at two different Reynolds numbers and a Prandtl number of 0.7. Note that this is the Prandtl number used in developing the Reynolds correlation. These comparisons are presented in Figure 5-2 for a Reynolds number of 20,000 and Figure 5-3 for a Reynolds number of 100,000. For comparison purposes, the EDSU correlation is also shown in both figures.

As can be seen, while there is a difference between Al-Arabi and Reynolds at the lower Reynolds number, that difference has essentially disappeared at the higher Reynolds number.

The EDSU correlation shows that the enhancement disappears faster than the other two correlations.

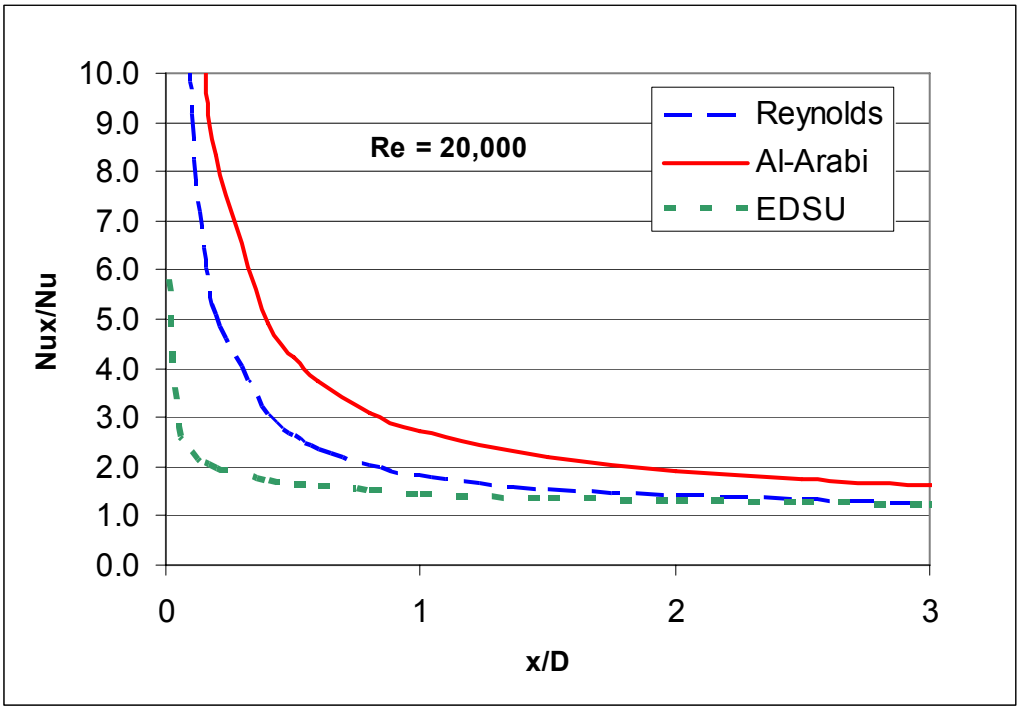

Figure 5-2
Performance of Three Correlations at a Reynolds Number of 20,000

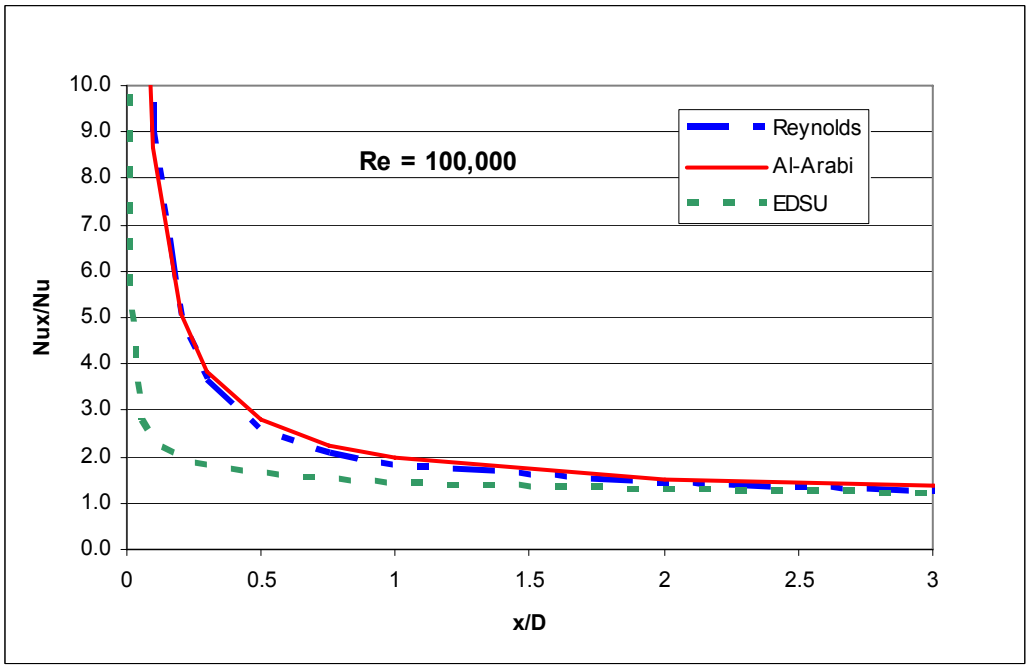

Figure 5-3
Performance of Three Correlations at a Reynolds Number of 100,000

5.7 Experimentally Based Correlations

In addition to the analytically based correlations described above, there also have been correlations developed from experimental data. Reference 14 describes a correlation attributed to McAdams. The form of this correlation is:

$$\frac{h_m}{h_\infty} = 1 + \frac{C}{\left(\frac{L}{D}\right)^n} \qquad (5\text{-}9)$$

Where:

h_m = mean heat transfer coefficient
C,n = constants depending on Reynolds and possibly Prandtl number

Reference 14 states that Equation 5-9 has been used to correlate some air heat transfer data at Prandtl number of 0.7 and Reynolds numbers between 26,000 and 56,000. For this case, C was equal to 1.4 and n was equal to 1.0.

These parameters were used to compare the McAdams correlation with the three analytically based ones. This comparison at a Reynolds number of 20,000 is presented in Figure 5-4. As can be easily seen, the results of this correlation are comparable with the other correlations.

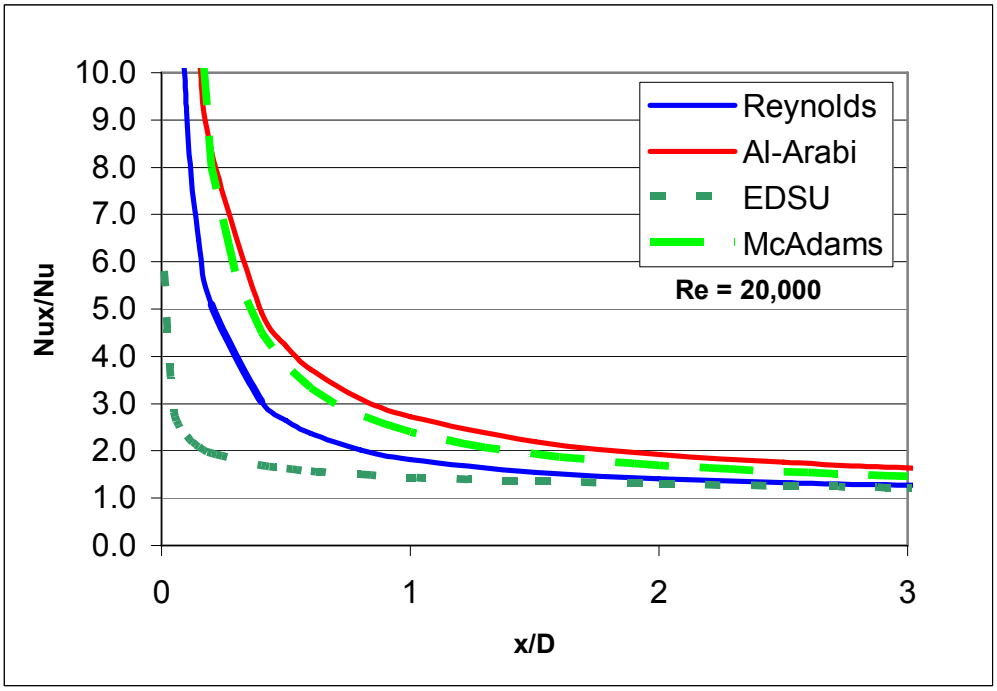

Figure 5-4
Comparison of the McAdams Correlation with Three Analytical Correlations

5.8 The Problem with Correlations

Examining the results of the previous section, it appears that the available correlations capture the process that is occurring in the entrance effect. However, it appears that using them is problematical for several reasons:

- The correlations are attempting to capture the enhancement (i.e., the improvement of mass transfer coefficient over fully developed) at the interface between the resistant material and the corroding material. Mathematically, this point represents a singularity as the mass transfer is related to the slope of the concentration profile which is discontinuous at the interface.
- The correlations predict enhancement factors on the order of 10 near the interface. Experience with FAC does not support such a large enhancement. Experience with heat transfer data suggests a lower enhancement factor see again Figure 4-5 and also see Deissler (reference 17) for more data. Although it should be noted that these experiments are difficult to perform. This subject is discussed at greater length in Appendix B.
- As stated by Coney, see Appendix A, the geometry of the area near the interface will change which in turn will impact the amount of enhancement.
- The use of a correlation which is based on an idealized mathematical analysis of the situation shown in Figure 4-3 implies the assumption that the entering flow is fully developed. In the practical situation this is not a reasonable assumption as there are always fittings, flow disturbances and corroding material upstream of the interface in question. It is likely, the flow entering the corroding material is not fully developed but in a transition state between the last upstream influence and fully developed.

  Further, even if the upstream is free of geometric influences, it is unknown how long a distance of resistant material upstream of the joint is necessary to produce a uniform concentration profile.

An approach to deal with these problems will be presented in the next section of this report.

6
DISCUSSION AND RECOMMENDATIONS

6.1 Discussion of the Implications of the Entrance Effect

Based on the information presented, the following conclusions about the entrance effect can be drawn:

- The entrance effect is a potential issue whenever non-resistant (susceptible) material is downstream of resistant material at least for single-phase flows.

  There has been no known work on the entrance effect in two-phase situations. From experience, particularly in cross-under lines, it has been observed that when an area in the large carbon steel pipe is locally patched, the area of degradation will move downstream. This experience was mentioned as long ago as 1981 by Richard Garnsey of CEGB (see the last paragraph of Section A.2).
- The exact determination of the degree of enhancement that will occur is a complicated function of the local geometry and the upstream conditions. It is probably not possible to capture an exact value the enhancement for a given situation of without complicated analysis. This analysis could be performed by using a computational fluid dynamics analysis of the joint and the upstream area.

6.2 Recommendations

6.2.1 For the Plant Owner

Based on the results of this work, it is recommended that:

- Plant operators identify and list areas where there are joints between resistant material upstream and non-resistant (susceptible) material downstream. This list should be considered in scheduling the downstream components for inspection. In performing these inspections particular attention should be paid in the areas immediately downstream of the connecting weld.
- Plant owners consider increasing the safety factor or placing into a separate inspection category the identified locations prone to the entrance effect.

6.2.2 For the FAC Community

Based on the results of this work, it is recommended that:

- If resources permit, non-plant specific computational fluid dynamic analysis be conducted. These analyses would be intended to provide guidance to the FAC engineer to allow prioritization of inspections. The objectives of this analysis would be to:

    - Determine how the enhancement factor varies with the length of the upstream, resistant material.

    - To examine the influence of Reynolds number on the enhancement obtained.

    - If possible examine the influence of an upstream fitting (e.g., an elbow).

- Further work be performed to identify when and under what conditions the entrance effect occurs under two-phase conditions.
- It is recommended that an enhancement factor of 2 be used as a placeholder in the next version of SFA to account for the entrance effect. This value is probably in the ballpark based on the heat transfer results and should highlight the occurrences of the entrance effect in the SFA results.

  If easily performed, it is recommended that the software flag in the output occurrences of non-resistant (susceptible) material downstream of resistant material. It should be noted that Version 2.2 of the Steam Feedwater Application (reference 2) has the ability to flag differences in chromium content between adjacent components.

7
REFERENCES

1. Chexal, B., et al., *Flow-Accelerated Corrosion in Power Plants*, EPRI, Palo Alto, CA: 1998, EPRI Report TR-106611-R1.
2. CHECWORKS™ Steam/Feedwater Application, Version 2.1, EPRI Report 1009600, October 2004.
3. Chexal, B., Horowitz, J.S., "Chexal-Horowitz Flow-Accelerated Corrosion Model – Parameters and Influences," presented at the Pressure Vessel and Piping Conference, Honolulu, Hawaii, 1995.
4. Horowitz, J.S., Chexal, B., Goyette, L.F., "A New Parameter in Flow-Accelerated Corrosion Modeling," PVP-Volume 368, ASME 1998.
5. Coney, M., *Erosion-Corrosion: The Calculation of Mass Transfer Coefficients*, CEGB Report RD/L/N 197/80, May 1981.
6. Goyette, L.F., Zysk, G.W., "Material Sampling in Erosion/Corrosion Programs," 1993, ASME PVP Vol. 259, Codes and Standards in a Global Environment.
7. Montgomery, Robert, personal communication, October 2007.
8. Barth, Andy, "V. C. Summer Unit #1, #1A Feedwater Heater," presented at the CHUG Meeting, Myrtle Beach, SC, January 2007.
9. Patulski, S. A., "Pleasant Prairie Unit 1 Feedwater Line Failure," report to EEI Prime Movers, April 1995.
10. Patulski, S.A., "Pleasant Prairie Unit 1 Feedwater Line Failure," presented at the International Joint Power Generation Conference, Minneapolis, October 1995.
11. Barth, A., "Main Steam Turbine Casing Drain, 3rd Stage Equalization 1" Diameter Pipe Break," presented at the CHUG Meeting, Charleston, SC, January 2005.
12. Goyette, L. F., "MSR Vent Condenser Drains Small Bore Piping Leak," presented at the CHUG Meeting Orlando, Florida, January 2006.
13. Berger, F. P., Hau, K.-F. F.-L, "Mass Transfer in Turbulent Pipe Flow measured by the Electrochemical Method," International Journal of Heat and Mass Transfer, Vol. 20, pp. 1185-1194, 1977.
14. Rohsenow, W. M. and Choi, H.Y., *Heat, Mass and Momentum Transfer*, Prentice-Hall, Englewood Cliffs, NJ, 1961.
15. Hartnett, J.P., "Experimental Determination of the Thermal Entry Length for the Flow of Water and Oil in Circular Pipes," *Trans. ASME*, 77:7, 1211, 1955.
16. Eckert, E.R.G. and Gross, J.F., *Heat and Mass Transfer*, McGraw Hill, 1963.
17. Deissler, R. G., "Turbulent Heat Transfer and Friction in the Entrance Regions of Smooth Passages," *Trans. ASME*, 77:7, 1221, 1955.
18. Hewitt, G.F., Shires, G.L., and Bott, T.R., *Process Heat Transfer,* CRC Press, Boca Raton, Florida, 1994.

19. Burmeister, L.C., *Convective Heat Transfer*, John Wiley, New York, 1993.
20. Kakaç, S., Shah, R.K., Aung, W., *Handbook of Single-Phase Convective Heat Transfer*, John Wiley, New York, 1987.
21. Al-Arabi, M., 1982. "Turbulent Heat Transfer in the Entrance Region of a Tube," *Heat Transfer Eng*., (3):76-83.
22. Hewitt, G. F., Shires, G. L., Bott, T. R., *Process Heat Transfer,* CRC Press, Boca Raton, Florida, 1994.

A
EARLY DESCRIPTIONS OF THE ENTRANCE EFFECT

This appendix will present some early descriptions of the entrance effect. Both of these descriptions were written by British researchers. Note that editorial notes are presented in square brackets (that is, [ ]).

A.1 Excerpt from Coney's Report (Reference A-1)

Reference A-1 is an extensive treatment of mass transfer coefficients and their role in FAC. In it, Coney described in clear terms the entrance effect:

> **"3.2 Developing Concentration Profiles**
>
> **If there is a discontinuity in the concentration or temperature at the wall of a smooth straight pipe, then the concentration or temperature profile in the boundary layer has to re-adjust itself over a certain finite length of tube. In the context of dissolution or of erosion-corrosion [now called FAC], this situation would arise at a joint between an insoluble or resistant material and a material which was soluble [non-resistant material]. The low concentration [of iron species] in the boundary layer encountering the start of the soluble surface causes an enhanced mass-transfer coefficient just downstream of the join[t]. We may call this 'mass-transfer entrance effect.'**
>
> **….**
>
> **"… In the practical context of a dissolving wall, the precise distribution of the mass-transfer coefficient following a change in material may not be too important, since as soon as a small amount is dissolved, a step will be formed causing local separation and thus a different mass-transfer behaviour [sic] …"**

Note that the second paragraph is particularly insightful as it recognizes that the geometry of the area immediately downstream of the connection will change as the carbon steel corrodes.

A.2 Excerpt from Garnsey's Letter

Richard Garnsey was a manager at the Central Electricity Generating Board. Apparently in the early 1980's he was visiting EPRI and wrote a memo discussing FAC. Two interesting quotes about the entrance effect were found in his letter, reference Figure A-2. Apparently, these quotes drew on Coney's work. The first of these quotations deals with single-phase flow:

"… This type of damage is usually attributed to the transition between tube and sleeve not being smooth enough. A step can enhance mass transfer coefficient by up to a factor of 2 over the plain straight tube. However, CERL[10] analysis and test data has shown that this is not the only or necessarily the major factor. The difference in the concentration of iron (or Cu^{2+}) ions in the boundary layer at the transition between sleeve and tube is critical. The boundary layer concentration of soluble iron will be less adjacent to the sleeve material that at the corresponding carbon steel surface hence at the transition between the sleeve and carbon steel the rate of dissolution of the magnetite [or] (Cu_2O) [if considering copper] on the carbon steel [or] (Cu alloy) will be higher. This has been demonstrated with dissimilar metal transition joints and at joints between 'perspex'[11] and 'plaster of paris' tubing.

"The most serious problems of this type which have developed in European nuclear plants have been on the Magnox, AGR, HTR, and Fast Reactor, ferritic steel tubed boilers just downstream of the orifice or ferrule assemblies at the boiler inlets. At this point mass transfer coefficient is increased by up to a factor of 3.5 over the smooth tube and rates of attack of several mm/year have been experienced. The solutions to the problem include, adding sleeves, inserting a section of austenitc tube between the orifice and the carbon steel tube, and changing water chemistry…."

Later on dealing with (mostly) two-phase conditions, he said:

"It is interesting to note that patching areas of damaged vessels and sections of pipework by buttering with erosion-corrosion [FAC] resistant materials has simply moved the problem to the edge of the buttered region. This is a further example of the reduction of the soluble iron concentration in the boundary layer adjacent to the intersection between materials of different solubility."

The behavior mentioned in the above paragraph has been seen particularly downstream of patch repairs made in cross under piping.

A.3 References

A-1 Coney, M., "Erosion-Corrosion: The Calculation of Mass Transfer Coefficients," CEGB Report RD/L/N 197/80, May 1981.

A-2 EPRI memo from Richard Garnsey (CEGB) to Daniel Cubicciotti (EPRI) August 31, 1981, subject "Erosion-Corrosion in Nuclear Powered Steam Supply Systems."

[10] CERL = Central Electricity Research Laboratory, part of the Central Electricity Generating Board in England.

[11] Perspex is usually known in the US by the trade names Plexiglas.or Lucite. Chemically it is Polymethyl methacrylate, a transparent plastic material..

B
MECHANISTIC EXPLANATION OF THE ENTRACE EFFECT

This appendix presents a less mathematical treatment of the entrance effect then is presented in the body of this report. This appendix is designed to be self-contained, so there will be few references to the body of this report.

B.1 Introduction

Flow-accelerated corrosion (FAC) is the name given to the degradation process that attacks carbon steel in the steam and feedwater system of conventional and nuclear power plants. In the simplest terms, FAC can be considered as the dissolution of the normally protective oxide film into a flowing stream of water or a water-steam mixture. FAC only occurs when the fluid is moving, when the fluid contains water and when the flow is unsaturated in iron. FAC can, in fact, be modeled as a turbulent mass transfer process. This was the approach taken by Berge and his co-workers at EDF.

The entrance effect in FAC occurs when a single-phase flow passes from a resistant material to a non-resistant material.[12] This effect is normally manifested by a groove downstream of the attachment weld between the corroding and the resistant material. (See Figure B-1 and additional photos in Section 3 of this report).

[12] This appendix will consider the entrance effect in single-phase (water) flows only. To my knowledge the subject of a similar entrance effect in two-phase (steam and water) flow has never been discussed at any length. Clearly such an effect would be dependent on the distribution of the water phase within the flow. The distribution of the phases is normally described by the term "flow regime."

A discussion of two-phase entrance effect is beyond the scope of this appendix.

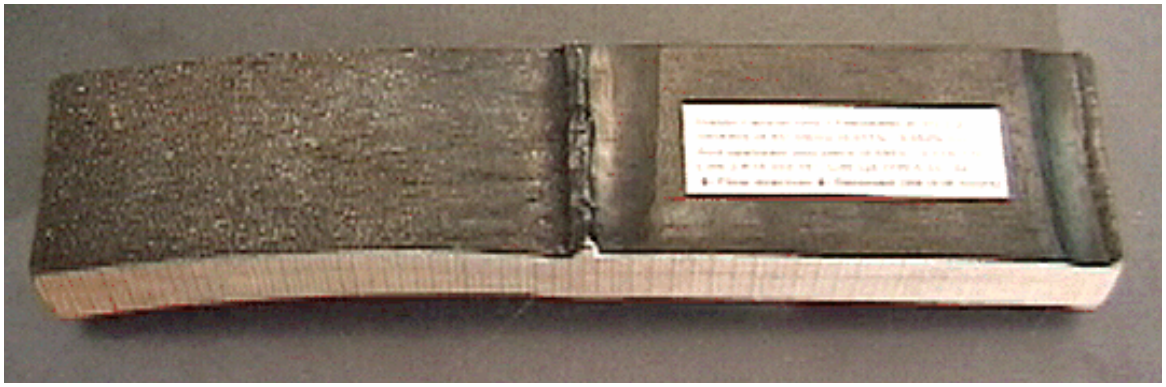

Figure B-1
Coupon Removed from Service at Diablo Canyon after 62,000 hours.
Flow direction is right to left.
(Photograph courtesy of Pacific Gas & Electric).

This effect is caused by the readjustment of the mass transfer concentration profile. As this is neither an obvious nor an intuitive phenomenon, this appendix will attempt to describe in physical terms what is occurring.

We will first describe turbulent flow. We will then make use of the analogy between turbulent heat transfer and turbulent mass transfer and describe the entrance effect in heat transfer terms. The discussion will then be extended to a simplified mass transfer example, and finally the real situation will be discussed.

B.2 Turbulent Flow

In the later part of the 19th Century the British scientist Osborne Reynolds first described the transition between turbulent and laminar flow as being a function of a dimensionless group of parameters. Reynolds observed that for a fluid flowing at a "low" velocity, the streamlines were parallel to each other and the flow did not mix along the length. This type of flow is called "laminar flow." At higher velocities, however, the flow became chaotic, and there were eddies in the flow stream that mixed the flow. This is called "turbulent flow." Reynolds defined a dimensionless number to characterize this transition.[13] This term is now known as the Reynolds number and is defined below:

$$\mathrm{Re} = \frac{\rho \cdot V \cdot D}{\mu} = \frac{W \cdot D}{\mu \cdot A} \qquad \text{(B-1)}$$

where:

Re = Reynolds number

[13] A **dimensionless number** is a quantity without any physical units and thus a pure number. Such a number is typically defined as a product or ratio of quantities which do have units, in such a way that all units cancel out.

ρ = Liquid density
V = Velocity
D = Diameter (or characteristic length)
μ = Viscosity
W = Flow rate
A = Cross sectional area.

For the case of a round pipe, equation (B-1) can be written as:

$$\mathrm{Re} = \frac{W \cdot D}{\mu \cdot A} = \frac{4 \cdot W}{\pi \cdot D \cdot \mu} \qquad \text{(B-2)}$$

In all cases, consistent units must be used to obtain a non-dimensional (i.e., unit-less number).

Originally Reynolds and later many other investigators have found that laminar flow in round tubes occurs at Reynolds numbers below about 2,300, and turbulent flow occurs above about 10,000. The regime in between is known as "transition flow" and is beyond the scope of this paper. Note that the Reynolds number in the feedwater system of a typical nuclear power plant is over 1,000,000.

In the 20th Century, the transport processes of turbulent flows were studied extensively. References B-1 & B-2, for example, present a great deal of background information on the turbulent processes we are concerned with in this paper. Some turbulent transport processes are presented in Table B-1.

Table B-1
Turbulent Transport Processes

Process	Typical Problem Solved
Momentum Transfer	The pressure distribution in a duct (normally the pressure drop between two points along the duct) or the drag on a moving body (e.g., automobile, golf ball).
Heat Transfer	The temperature on the wall and the rate of heat transfer to or from the wall (e.g., in a heat exchanger).
Mass Transfer	The concentration profile and the rate of mass transfer to or from the wall (e.g., in a cooling tower, an industrial dryer).

Dating back to the earliest work in the field of turbulent transport processes, the concept of analogies between and among the processes has been employed. A number of well-known analogies have been defined and are in wide use (see again References B-1 & B-2). For our purposes, it is sufficient to realize that in qualitative sense that the processes of heat transfer and mass transfer are analogous.

Remembering that FAC can be considered as turbulent mass transfer, we will first consider an analogous example from heat transfer. This is being done because most people have an easier time visualizing temperatures and heat flows than concentrations and mass flows. When we have finished this description, we will then present a simple mass transfer example, and finally redo the argument for the case of FAC.

B.3 Heat Transfer Analogy

Let us consider the situation as shown in Figure B-2. In this case there is a fluid flowing along in a straight, insulated tube. At the point x=0, the insulated tube becomes a heated tube. Let us examine the rate of heat transfer along the tube.

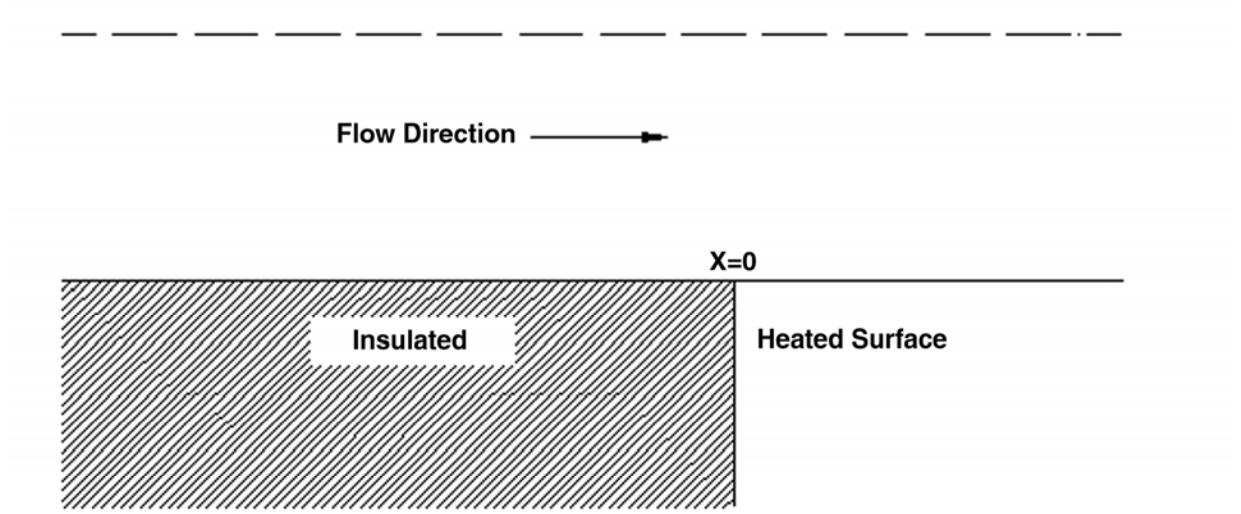

Figure B-2
Heat Transfer Analogy to the Entrance Effect

Now let us consider the temperature profile at three locations along the above case. At a location before x=0, the temperature profile is uniform. For a flow at speeds well below the sound speed of the fluid, the case we are considering, then the temperature profile must be uniform.[14] Note that even though there is a velocity profile (ranging from zero at the surface to a maximum value at the centerline), the temperature is uniform across the section. (See Figure B-3).

Now let us consider the temperature profile at a point well downstream of x=0. At this location, the temperature profile can be considered as fully developed turbulent. For the case we are

[14] This proviso is necessary because at very high speeds, aerodynamic heating occurs. This is significant at speeds approaching and exceeding the sound speed. As the sonic velocity in water is about 4,000 feet per second, this is a safe assumption for feedwater systems.

considering, a heated wall, this means that the temperature will be a maximum at the wall and fall off toward the centerline. (See again Figure B-3).

Finally, let us consider a location just downstream of location x=0. There the temperature profile will be neither uniform nor fully developed. Obviously, there must be a transition area where the temperature profile develops.[15] (See again Figure B-3).

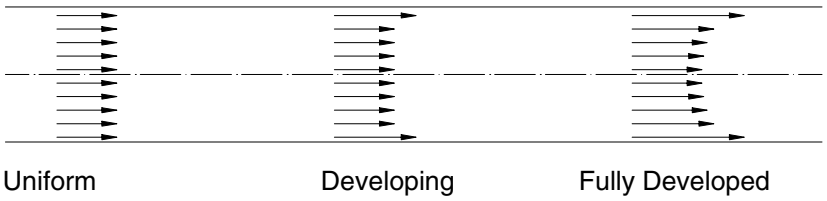

Figure B-3
Temperature Profiles

Once we understand the development of the temperature profiles, we can understand what is happening with the heat transfer. The rate of heat transfer to the fluid can be written as:

$$\frac{Q}{A} = -k \cdot \left(\frac{\partial T}{\partial z} \right)_{wall} \qquad \text{(B-3)}$$

where

Q	= rate of heat transfer
A	= Area of the wall
k	= thermal conductivity of the fluid
T	= temperature
z	= direction into the fluid

In words this says that the rate of heat transfer per unit area is proportional to the thermal conductivity of the fluid (a physical property) and the temperature gradient at the wall.

With this information, let us consider the temperature profiles discussed above. In the upstream case there is no heat transfer because the temperature gradient at the wall is zero. This is obvious. But what is a little less obvious is the fact that the developing temperature gradient at the wall is always greater than the fully developed temperature gradient. This fact means that there will be an increase from the fully developed heat transfer.

There have been various heat transfer experiments done to establish the above claim. For example, Figure B-4 presents the experimental data of Harnett, Reference B-3. Note that this

[15] Note that in the cases we are considering, the velocity profile is always considered fully developed. This may not be true in the actual case, but will be assumed here for the sake of illustration.

data is for oil (Prandtl number between 60 and 480). The same paper presents similar data for water (Prandtl number between 6.5 and 8.0). Further, Deissler (reference B-4) presents similar experimental data (taken by others) for air (Prandtl number ~ 0.7).

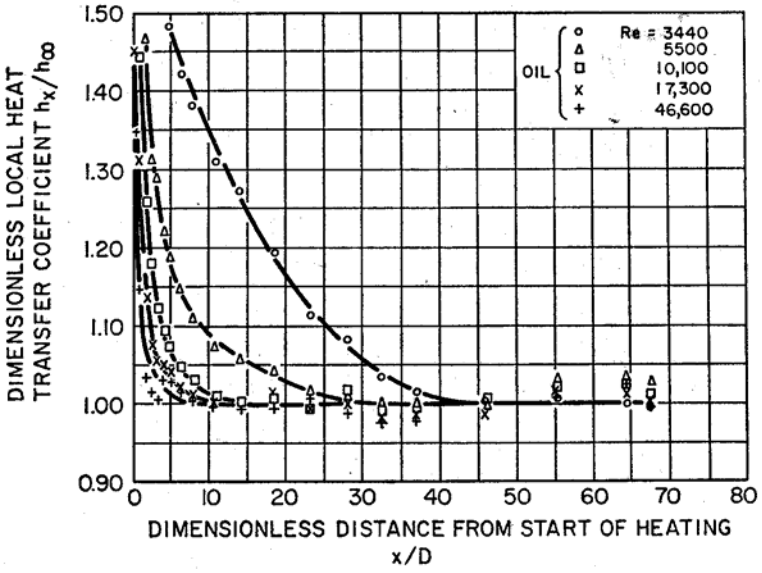

Figure B-4
Thermal Entrance Effect, Data of Hartnett (Reference B-)

Some conclusions and generalizations may be drawn from Figure B-4.

- There is an obvious enhancement due to the thermal entrance.
- Although the maximum Reynolds number presented (46,600) is small compared to feedwater piping, the trend with Reynolds number seems apparent. The higher the Reynolds number the shorter the effect of the entrance. For the Reynolds numbers of interest the maximum duration of this effect is probably under one diameter downstream of the resistant material.
- The improvement in heat transfer coefficient shown appears to be a maximum of about 50% (i.e., the heat transfer coefficient ratio is 1.5). It should be strongly stressed that in experiments of this type the determination of the maximum heat transfer coefficient will normally be lower than the maximum because of axial conduction in the test section. Further, these tests are normally concerned about large-scale enhancements (say on the order of a pipe diameter). We are concerned about a smaller scale. A more reasonable value for the maximum enhancement is probably at least 2.

Reference B-1 states that Equation B-4 has been proposed by McAdams to correlate the various experimental data.

$$\frac{h_x}{h_\infty} = 1 + \frac{C}{(L/D)^n} \qquad \text{(B-4)}$$

where:

h_x = the local heat transfer coefficient
h_∞ = the fully developed heat transfer coefficient
L/D = Length to diameter ratio
C,n = Constants[16] which are a function of geometry, Reynolds number and possibly the Prandtl number.[17]

Note that Equation B-4 predicts very large enhancements at L/D ratios of less than unity. Again, this is not surprising as a very large temperature gradient at the wall exists at x=0.

B.4 Mass Transfer Analogy

With the heat transfer analogy as background, let us know consider an idealized mass transfer analogy. As before we will consider a situation where the velocity field is fully developed and the concentration profile is developing. Physically we are dealing with the same situation as already presented in Figure B-2. A material that does not dissolve is followed by another material, which will readily dissolve. Let us consider the simplest case in which there is no dissolved material in the flow at the entrance to the test section (x=0). To make the example even more concrete, let us assume that the fluid is hot water, the upstream material is plastic, the downstream material is made of compressed sugar, and that there is no sugar present (i.e., dissolved) in the water entering into the test section.

With these assumptions let us now examine the concentration profiles upstream, far downstream and just downstream of x=0. These concentration profiles are presented in Figure B-5

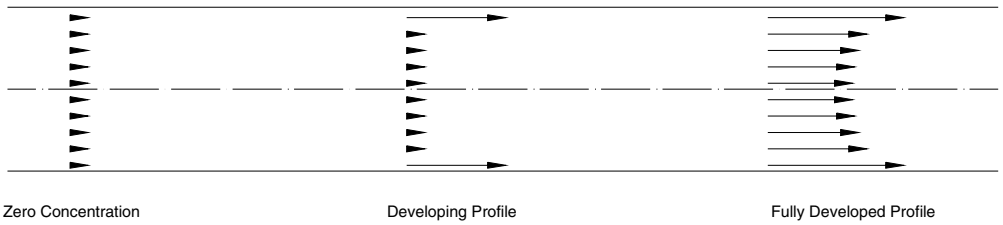

Figure B-5
Concentration Profiles

As the concentration profiles of Figure B-5 are so similar to the temperature profiles of Figure B-3, a similar behavior between the two cases should be expected. That is a local increase in the mass transfer (i.e., the amount of dissolution) of the sugar immediately downstream of the sugar-plastic interface. This implies that the cross section of the test section after some duration would look approximately like Figure B-6.

[16] In one example correlation given in Reference B-1, C was 1.4, and n was 1.

[17] The Prandtl number is a dimensionless number that relates the viscous diffusion to the thermal diffusion of a fluid. It is a property of the fluid. See References B-1, B-2 or any textbook on heat transfer for more information.

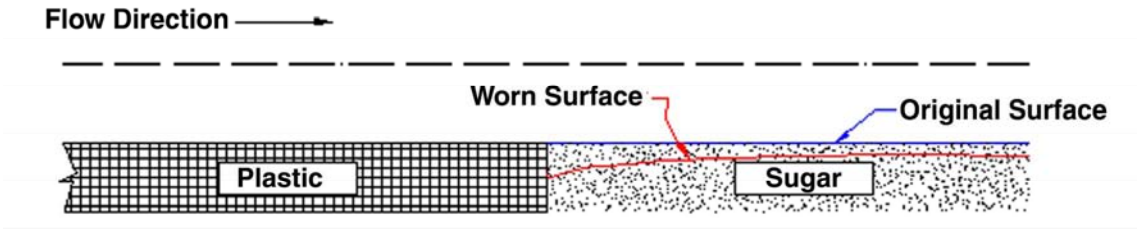

Figure B-6
Schematic of Worn Sugar Surface

We are now fairly close to describing the entrance effect seen in, for example, Figure B-1 and compare it with the schematic representative presented in Figure B-6.

B.5 The Real Situation

The real situation is more complicated than the sugar example presented above for several reasons. Let us discuss these reasons and what role they may play in the "real world."

- Non-zero entering concentration – in the above illustration, the sugar concentration (analogous to the dissolved iron concentration) was assumed to be zero. In the feedwater system this concentration would certainly be greater than zero. However, studies have shown that the iron concentrations in the condensate and feedwater systems are low enough that the difference between the wall concentration and the free-stream concentration do not change greatly along the flow path.[18] Thus, the presence of dissolved iron should have no impact on the above conclusions.[19]
- Non-fully-developed velocity distribution – we have here-to-fore assumed that the velocity profile is fully developed. This may not be so at all locations of interest, particularly if there are nearby, upstream fittings present. This would impact the severity and the geometry of the accelerated attack found, but the fundamental conclusion as to why the additional degradation is taking place would not be affected.
- Influence of the weld – looking again at Figure B-1 it is apparent that the additional attack occurred a very short distance downstream from the weld. This may have been caused by the weld metal migration or the heat affected zone of the weld reducing the inherent rate of FAC. Either of these reasons explains why Figure B-1 and the sketch shown in Figure B-6 do not completely agree. However, the influence of the weld extends only a very small distance downstream of the weld.

  Also, in extreme cases, the weld material may be undercut by the localized attack. This would exacerbate the degradation caused by the combination of FAC and the entrance effect.

---

[18] The difference between the wall concentration (the iron solubility) and the free stream iron concentration is the driving force for the mass transfer process. That is why it is the important parameter is discussing the impact of iron concentration in the water.

[19] This assumes that the iron concentration is less than the saturation value. This is a good assumption in the feedtrain. It may be a bad assumption in the steam generator blowdown system, and in the lower portions of a recirculating steam generator.

- Galvanic effect caused by the contact of dissimilar metals – it is often speculated that we call the "entrance-effect" is really galvanic corrosion. This contention can be easily disproved by the observation that the carbon steel is always worn on the upstream end. The downstream carbon steel to resistant material weld area is never affected in the same manner.

B.6 Why Do We Care

One might argue that the impact of the entrance effect is real, but not worthy of attention as it only a small area of the component affected.

Unfortunately, experience has shown that this argument is incorrect. The thinning is indeed localized, but this may serve to weaken a component at its thinnest point – at the point of attachment. This localized thinning may require a fitting to be replaced. Further, it is speculated that the entrance effect contributed to the failure at the Pleasant Prairie Power Plant in February 1995. This failure was the guillotine break of a feedwater line immediately downstream of a tee that contained more than 0.1% chromium. If the entrance effect produce the characteristic grooving immediately downstream of the attachment weld, then a guillotine rupture would be likely.[20]

B.7 Further Information

This appendix is essentially an expansion of reference B-5. This reference should be consulted for a more rigorous discussion. Additional information may be found in standard heat transfer or mass transfer books. Also, Coney (reference B-6) and Coney et al. (reference B-7) present additional, relevant information.

B.8 References

B-1. Rohsenow, W. M. and Choi, H.Y., *Heat, Mass and Momentum Transfer*, Prentice-Hall, Englewood Cliffs, NJ, 1961.

B-2. Kreith, F., *Principles of Heat Transfer*, International Textbook Company, Scranton, PA, 1965.

B-3. Hartnett, J.P., "Experimental Determination of the Thermal Entry Length for the Flow of Water and Oil in Circular Pipes," *Trans. ASME*, 77:7, 1211, 1955.

B-4. Deissler, R. G., "Turbulent Heat Transfer and Friction in the Entrance Regions of Smooth Passages," *Trans. ASME*, 77:7, 1221, 1955.

B-5. Horowitz, J.S., Chexal, B. & Goyette, L.F., "A New Parameter in Flow-Accelerated Corrosion Modeling," PVP-Volume 368, ASME 1998.

B-6. Coney, M., "Erosion-Corrosion: The Calculation of Mass Transfer Coefficients," CEGB Report RD/L/N 197/80, May 1981.

[20] Unfortunately, the detailed information about the Pleasant Prairie rupture has been closely held due to litigation arising from the accident.

B-7. Coney, et al., “Thermal-Hydraulic Effects on Mass Transfer Behaviour and on Erosion Corrosion Metal Loss Rates,” CEGB, TPRD/L/2349/N82.

C
BOUNDARY LAYER ANALYSIS

This appendix will present an alternate description of the entrance effect using the concept of a boundary layer. This description will avoid most of the mathematics involved in a very difficult subject. Note that this material does not contradict, but merely restates from a different point-of-view the material previous presented.

As in the previous discussions, we will begin describing hydrodynamics, move to heat transfer, and finally cover mass transfer.

C.1 Hydrodynamic Boundary Layer

C.1.1 Background

The concept of the hydrodynamic boundary was defined by Ludwig Prandtl in 1904. The concept was developed to simply the problem of computing a drag on a body in an infinite medium. Essentially, the flow is divided into two parts:

- The portion of the flow near the body that is influenced by the body – the boundary layer. In the boundary layer friction is important, and
- The portion of the flow far enough away from the body as to be not influenced by it – the free stream. In the free stream, the fluid is considered ideal (i.e., it does not have viscosity).

These simplifications have had far reaching implications through fluid mechanics and related fields.

The development of the boundary layer on a flat plat is illustrated in Figure C-1.

C.1.2 Boundary Layer over a Flat Plate

To explore the nature of boundary layers, let us consider the simplest example, the laminar flow over a flat plate at zero angle of incidence. This situation is shown in Figure C-1. In practice, the edge of the boundary is taken as the location where the velocity reaches 99% of the free stream velocity. The boundary layer is shown as the broken line in the figure. The height of the boundary layer is indicated with the symbol δ. The velocity profile within the boundary layer is also shown in the figure.

If the flow continues over the same plate, a point will reach when the boundary layer changes from laminar to turbulent. In doing so, it passes through a transition region. This behavior is illustrated in Figure C-1. The location of the transition to turbulent boundary layer has been

found to be at a length Reynolds number between about 320,000 and 1,000,000 depending on the turbulence in the free stream. The length Reynolds number is defined as:

$$\mathrm{Re}_x = \frac{V_\infty \cdot x}{\nu} \qquad \text{(C-1)}$$

where:

Re_x = length based Reynolds number
V_∞ = free stream velocity
x = distance from the leading edge
ν = kinematic viscosity, $\nu = \mu / \rho$.

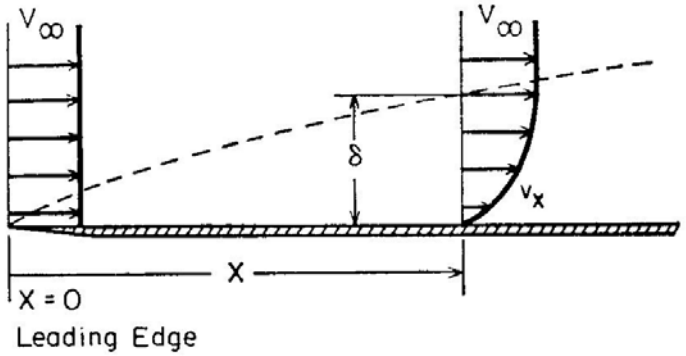

Figure C-1
Laminar Boundary Layer over a Flat Plate from Reference C-1

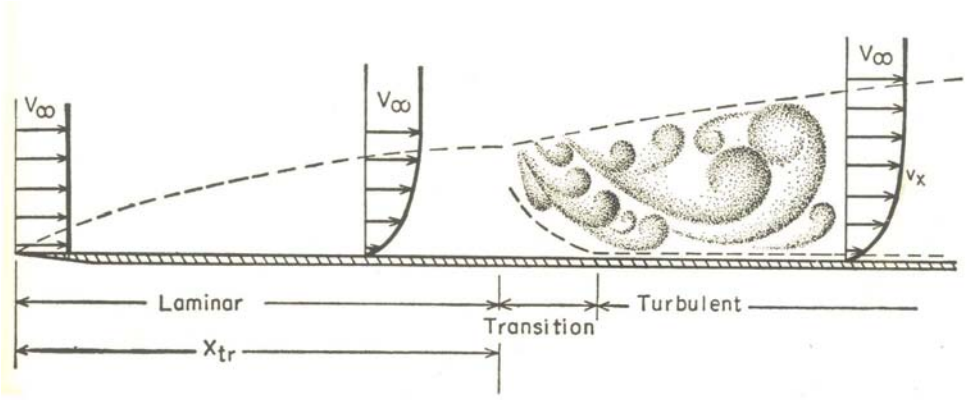

Figure C-2
Development of Laminar and Turbulent Boundary Layers over a Flat Plate from Reference C-1

C.1.3 Boundary Layer in Entrance Regions

The entry region in various geometries can be solved using the boundary layer approach. For example, the problem of defining the velocity distribution and the pressure drop in the entrance region of infinite parallel plates, and round tubes have been solved for laminar and turbulent flows.

For example, Figure C-3 presents the calculated velocity profiles for laminar flow at the entrance to the circular pipe presented in terms of dimensionless distance from the entrance. The velocity profile changes from a slug shape at the inlet to the fully developed parabolic profile. Note the dimensionless distance may be re-written as:

$$\frac{\nu \cdot x}{r_o^2 \cdot V_o} = \frac{x}{r_o} \cdot \frac{1}{\mathrm{Re}_r} \qquad \text{(C-2)}$$

Where:

r_o = radius of pipe

Re_r = Reynolds number based on pipe radius

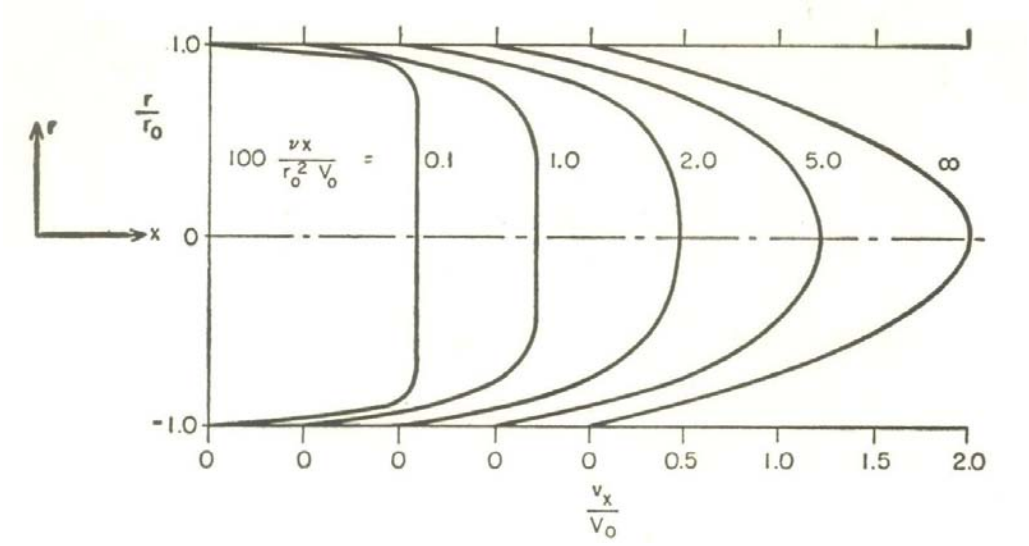

Figure C-3
Velocity Distribution for Laminar Flow in the Entrance Region of a Circular Pipe from Reference C-1

Further information about hydrodynamic boundary layers may be found in classic books on the subject especially reference C-2. Reference C-3 provides a more in depth, much more mathematical treatment of the subject.

C.2 Thermal Boundary Layer

In considering heat transfer problems with flow, the concept of a thermal boundary layer is also useful. In fact, the treatment of thermal boundary layers is quite similar to hydrodynamic ones. The principal difference in the formulation is that the temperature is represented by a dimensionless variable[21]. For example, if the fluid of free stream temperature of T_∞ comes in contact with a wall at temperature of T_w, then the dimensionless temperature (Θ) is written as:

$$\Theta = \frac{(T - T_w)}{(T_\infty - T_w)} \qquad \text{(C-4)}$$

The edge of the boundary level is normally taken as when the dimensionless temperature (i.e.,Θ) reaches 99%.

Investigators such as Deissler (reference C-4), have solved the thermal entrance problem for laminar and turbulent flow for a variety of geometries and entrance conditions. As the resulting solutions normally involve infinite series, these solutions are normally put into a more useable form by correlating with various dimensionless variables (e.g., Reynolds number, Prandtl number, L/D).

C.2.1 Developing Thermal Boundary Layer at the Inlet of a Tube

Let us know consider the behavior of a laminar, thermal boundary layer at the entrance to a circular tube. Consider Figure C-4, and notice the three temperature profiles shown.

- The first profile shows a uniform temperature distribution at the entrance. The thickness of the thermal boundary layer (indicated as δ_T) is zero.
- The second profile shows a developing condition. The thermal boundary layer has not reached the center of the pipe, and the temperature profile is flat in the middle. As will be seen in the next bullet, the fully developed laminar profile is parabolic without a flat spot in the center.
- The third profile indicated that fully developed conditions have been attained. The thermal boundary layer no longer exists, and the temperature distribution is parabolic (again for laminar flow).

[21] In fact, the hydrodynamic boundary layer is defined with a dimensionless variable, namely the ratio of local to free stream velocity.

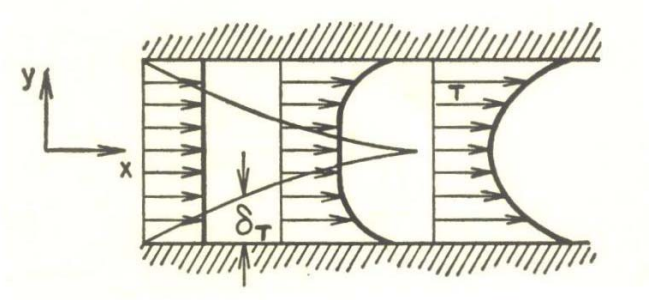

Figure C-4
Developing Thermal Boundary Layer for Laminar Flow at the Entrance to a Tube from Reference C-1

Now the point of this exercise is to state that the heat transfer through a laminar thermal boundary layer is simply the heat conduction through the boundary layer. Therefore, for a uniform wall temperature, the heat transfer through the boundary layer is equal to conduction through the boundary layer, or:[22]

$$Q'' \sim \frac{(T_w - T_\infty)}{\delta_T} \qquad \text{(C-5)}$$

where:

Q'' = heat flux

The significance of Equation C-5 is that the heat transferred varies inversely with the thickness of the thermal boundary layer. Thus, considering again Figure C-4, the heat transfer starts at a very high value and decreases with distance from the entrance. Thus, the entrance effect is a result of the growth of the thermal boundary layer.

Although the above conclusion is true for laminar flow, similar results are also true for other flow situations (e.g., laminar transitioning to turbulent, or all turbulent flow).

C.2.2 Influence of Prandtl Number

In general the shapes of the hydrodynamic and thermal boundary layers are similar. However, unless the Prandtl number is unity, the two boundary layers will grow at different rates. Consider laminar flow over a heated plate. If there are no thermal entry length, Reference C-1 presents the relationship between the thicknesses of these two boundary layers with Prandtl number as:

$$\frac{\delta_T}{\delta} = \frac{1}{1.026 \cdot \sqrt[3]{\mathrm{Pr}}} \qquad \text{(C-6)}$$

[22] There are various conditions on this argument, but for the sake of illustration, they will not be presented here.

Thus, the ratio of boundary layer thicknesses varies with the Prandtl number.

- If the Prandtl number is smaller than unity, the thermal boundary layer will be thicker than the hydrodynamic one.
- On the other hand, the thermal boundary layer will be thinner than the hydrodynamic one.

C.3 Concentration or Mass Transfer Boundary Layer

The same considerations that apply to the thermal boundary layer also apply to the mass transfer or concentration boundary layer. Consider Figure C-5, the concentration boundary layer forming over a flat plate. The thickness of the concentration boundary layer is shown by the solid line. The thickness of the concentration boundary layer is denoted by δ_c. Note that the situation depicted in this figure also depicts a steel surface corroding in a moving flow.

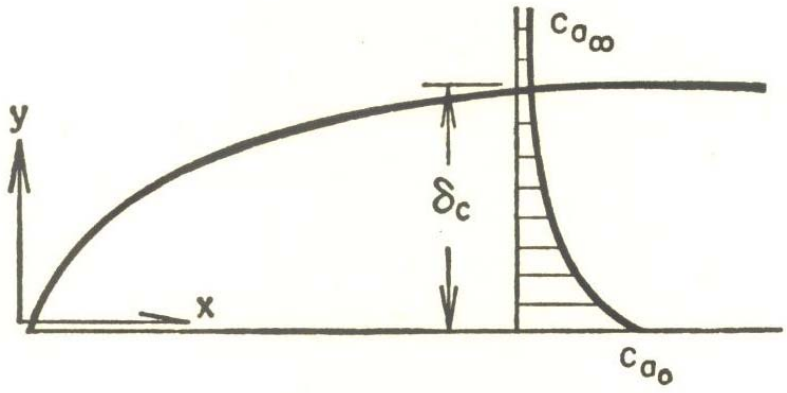

Figure C-5
Concentration Boundary Layer over a Flat Plate from Reference C-1

As was the case of the thermal boundary layer, the thickness is defined in dimensionless terms as:

$$0.99 = \frac{(c_{a0} - c_a)}{(c_a - c_{a\infty})} \qquad \text{(C-7)}$$

where:

c_{a0} = concentration of species "a" at the wall
c_a = concentration of species "a" at an arbitrary location
$c_{a\infty}$ = concentration of species "a" at the wall

As is the case with the thermal boundary layer, the relative thickness of the concentration boundary layer is governed by the Schmidt number.

- If the Schmidt number is smaller than unity, the concentration boundary layer will be thicker than the hydrodynamic one.
- On the other hand, the concentration boundary layer will be thinner than the hydrodynamic when the Schmidt number is greater than one.

C.3.1 Concentration Boundary Layer and the Entrance Effect

Consider again Figure C-5. This figure can be viewed as representing the entrance to a pipe showing a developing concentration boundary layer. Once again, it can be argued that in the entrance region, the rate of mass transfer varies inversely with the thickness of the concentration boundary layer. Thus, the mass transfer varies from an undefined value at the entrance (where the boundary layer is of zero thickness) to the fully developed value after the boundary layer disappears.

C.4 Closure

This appendix has described the entrance effect in terms of boundary layer theory. While this description is different from the descriptions presented in the body of this report and of Appendix B, the physics of the process are the same.

C.5 References

C-1. Rohsenow, W. M. and Choi, H. Y., *Heat, Mass and Momentum Transfer*, Prentice-Hall, Englewood Cliffs, NJ, 1961.

C-2. Prandtl, L. and Tietjens, O. G., *Applied Hydro- and Aeromechanics*, McGraw Hill, 1934.

C-3. Schlichting, H. et. al, *Boundary Layer Theory, 8th Edition,* McGraw Hill, 2004.[23]

C-4. Deissler, R. G., "Turbulent Heat Transfer and Friction in the Entrance Regions of Smooth Passages," *Trans. ASME*, 77:7, 1221, 1955.

[23] Other, older editions are probably still available.

Export Control Restrictions

Access to and use of EPRI Intellectual Property is granted with the specific understanding and requirement that responsibility for ensuring full compliance with all applicable U.S. and foreign export laws and regulations is being undertaken by you and your company. This includes an obligation to ensure that any individual receiving access hereunder who is not a U.S. citizen or permanent U.S. resident is permitted access under applicable U.S. and foreign export laws and regulations. In the event you are uncertain whether you or your company may lawfully obtain access to this EPRI Intellectual Property, you acknowledge that it is your obligation to consult with your company's legal counsel to determine whether this access is lawful. Although EPRI may make available on a case-by-case basis an informal assessment of the applicable U.S. export classification for specific EPRI Intellectual Property, you and your company acknowledge that this assessment is solely for informational purposes and not for reliance purposes. You and your company acknowledge that it is still the obligation of you and your company to make your own assessment of the applicable U.S. export classification and ensure compliance accordingly. You and your company understand and acknowledge your obligations to make a prompt report to EPRI and the appropriate authorities regarding any access to or use of EPRI Intellectual Property hereunder that may be in violation of applicable U.S. or foreign export laws or regulations.

The Electric Power Research Institute (EPRI)

The Electric Power Research Institute (EPRI), with major locations in Palo Alto, California; Charlotte, North Carolina; and Knoxville, Tennessee, was established in 1973 as an independent, nonprofit center for public interest energy and environmental research. EPRI brings together members, participants, the Institute's scientists and engineers, and other leading experts to work collaboratively on solutions to the challenges of electric power. These solutions span nearly every area of electricity generation, delivery, and use, including health, safety, and environment. EPRI's members represent over 90% of the electricity generated in the United States. International participation represents nearly 15% of EPRI's total research, development, and demonstration program.

Together…Shaping the Future of Electricity

Printed on recycled paper in the United States of America

1015072

Electric Power Research Institute
3420 Hillview Avenue, Palo Alto, California 94304-1338 • PO Box 10412, Palo Alto, California 94303-0813 • USA
800.313.3774 • 650.855.2121 • askepri@epri.com • www.epri.com